MARTIN MARIETTA ENERGY SYSTEMS LIBRARIES
3 4456 0365446 3

ORNL-3443
UC-40 – Radiation Effects on Materials
TID-4500 (19th ed., Rev.)

ANNEALING OF GAMMA RAY INDUCED CHANGES IN ANTIMONY DOPED GERMANIUM

Jay Cee Pigg

CENTRAL RESEARCH LIBRARY
DOCUMENT COLLECTION
LIBRARY LOAN COPY
DO NOT TRANSFER TO ANOTHER PERSON
If you wish someone else to see this document, send in name with document and the library will arrange a loan.

OAK RIDGE NATIONAL LABORATORY
operated by
UNION CARBIDE CORPORATION
for the
U.S. ATOMIC ENERGY COMMISSION

Printed in USA. Price: $2.25 Available from the
Office of Technical Services
U. S. Department of Commerce
Washington 25, D. C.

LEGAL NOTICE

This report was prepared as an account of Government sponsored work. Neither the United States, nor the Commission, nor any person acting on behalf of the Commission:

A. Makes any warranty or representation, expressed or implied, with respect to the accuracy, completeness, or usefulness of the information contained in this report, or that the use of any information, apparatus, method, or process disclosed in this report may not infringe privately owned rights; or

B. Assumes any liabilities with respect to the use of, or for damages resulting from the use of any information, apparatus, method, or process disclosed in this report.

As used in the above, "person acting on behalf of the Commission" includes any employee or contractor of the Commission, or employee of such contractor, to the extent that such employee or contractor of the Commission, or employee of such contractor prepares, disseminates, or provides access to, any information pursuant to his employment or contract with the Commission, or his employment with such contractor.

ORNL-3443

Contract No. W-7405-eng-26

SOLID STATE DIVISION

ANNEALING OF GAMMA RAY INDUCED CHANGES IN ANTIMONY DOPED GERMANIUM

Jay Cee Pigg

DATE ISSUED

MAY 14 1963

Submitted as a thesis to the Graduate Council of the University of Tennessee in partial fulfillment of the requirements for the degree Doctor of Philosophy

OAK RIDGE NATIONAL LABORATORY
Oak Ridge, Tennessee
operated by
UNION CARBIDE CORPORATION
for the
U.S. ATOMIC ENERGY COMMISSION

MARTIN MARIETTA ENERGY SYSTEMS LIBRARIES

3 4456 0365446 3

ACKNOWLEDGMENTS

The advice and assistance of the members of the Solid State Division of the Oak Ridge National Laboratory has contributed greatly to the success of this work. Particular thanks are due to Dr. J. H. Crawford, Jr., for his encouragement and guidance throughout this research. Drs. H. C. Schweinler, D. K. Holmes, and M. T. Robinson have been of particular assistance. The help of Mr. E. G. Craig who assisted in construction of the instrumentation was essential to the completion of the work. The outstanding help of Mrs. G. M. Warren in preparing the manuscript is greatly appreciated.

Special thanks are due the members of the author's graduate committee, in particular the chairman, Dr. J. O. Thompson. The encouragement and assistance of the members of the Physics Department of the University of Tennessee are gratefully acknowledged.

TABLE OF CONTENTS

CHAPTER		PAGE
I.	INTRODUCTION	1
II.	EXPERIMENTAL PROCEDURE	9
III.	EXPERIMENTAL RESULTS	29
	Isochronal Survey of Carrier Concentration Annealing	29
	Isothermal Anneal of Carrier Concentration	34
	Mobility Changes	41
	Temperature Dependence of Observed Change in Carrier Concentration	54
IV.	DISCUSSION	61
	Summary of Experimental Results	61
	Interpretation of the Data	67
	Possible Models	71
	Antimony-Vacancy and Antimony-Divacancy Model	73
	Other Possible Models	93
	The 0.09 ev Level	93
V.	SUMMARY	95
BIBLIOGRAPHY		99

LIST OF FIGURES

FIGURE PAGE

1. Sample Configuration. 16
2. Sample Holder 20
3. Schematic of Temperature Control Furnace in Measuring Position. 22
4. Measuring Circuit Schematic 25
5. Isochronal Anneal EP8-A 30
6. Isochronal Anneal Data of Brown, Augustyniak, and Waite 31
7. Isochronal Anneal of EP8-K. 33
8. Summary of Isothermal Annealing Curves Measured at $77^{\circ}K$. 35
9. Log of $\tau_{\frac{1}{2}}$ vs $\frac{10^3}{T}$ for the $77^{\circ}K$ Measurement. 38
10. Saturation Plateaux at $77^{\circ}K$ 40
11. Isothermal Anneal at $377.2^{\circ}K$ EP8-P 42
12. Isothermal Anneal EP8-J. 43
13. Isothermal Anneal EP8-O 44
14. Isothermal Anneal EP8-Q. 45
15. Isothermal Anneal EP8-M. 46
16. Isothermal Anneal EP8-B. 47
17. Isothermal Anneal EP8-E. 48
18. Isothermal Anneal EP8-F. 49
19. Isothermal Anneal EP8-G 50
20. Isothermal Anneal EP8-I. 51

FIGURE PAGE

21. Composite $\tau_{\frac{1}{2}}$ 52

22. Isochronal anneal EP8-K 53

23. Log $\frac{1}{\mu}$ vs log T for EP8-P. 55

24. Isothermal Anneal of Reciprocal Mobility. 56

25. Carrier Concentration Removed vs Co^{60} Gamma Irradiation 58

26. Effect of Irradiation and Anneal on the Hall Constant EP8-P. 59

27. Fit of Data by an Approximated Equation 90

ABSTRACT

An investigation of the annealing of the radiation induced carrier concentration change in antimony doped germanium in the temperature range between 370° Kelvin and 455° Kelvin has been made. The irradiations were conducted at liquid nitrogen temperature using cobalt-60 gamma irradiation. A model which explains the observed behavior is presented. On the basis of this model, the observed annealing consists of vacancy diffusion simultaneously to impurity sites and annihilation centers. Analysis of the activation energy for the annealing process yields values of 0.8 to 1.4 electron volts in agreement with the range of energies which have been attributed to vacancy motion but which cannot be resolved into unique components. The complex activation energy is explained by the model in terms of the impurity concentration. It is observed that the change in carrier concentration saturates before complete annealing is achieved. This saturation which is stable for further annealing at higher temperatures is also explained in terms of the model. The vacancies are considered to diffuse to annihilation centers, such as dislocation lines, and to the site adjacent to an antimony atom. Those which go to an antimony are trapped. The antimony-vacancy complex can break up to supply a vacancy back to the system or can trap an additional vacancy producing an antimony-divacancy complex. The antimony-divacancy complex is stable for the temperature range considered. The antimony-vacancy reaction comes into equilibrium very quickly compared to the annihilation process.

CHAPTER I

INTRODUCTION

The electrical properties of semiconductors are known to be extremely sensitive to both the chemical impurity and the structural imperfections present in the crystal.[1] Consequently, a change in the imperfection content of the crystal will produce a change in its electrical properties. Such imperfections may consist of chemical impurities situated at a lattice site or some interstitial position,[2] or they may consist of discontinuities in the periodicity of the lattice.[3]

Lattice imperfections, or defects, may be introduced in various ways.[4] Some of the techniques employed are plastic deformation, quenching, and irradiation. Irradiation is the most flexible of these three techniques for introducing lattice defects since it is subject to precise control and measurement. The detailed nature of the defects introduced by these methods differ greatly. Hobstetter and Renton found that the

---

[1] W. Shockley, Electrons and Holes in Semiconductors. (D. Van Nostrand Company, New York, 1950), pp. 4-26, 250-294.

[2] W. Crawford Dunlap, Jr., "Impurities in Germanium," Progress in Semiconductors, A. F. Gibson (ed.), Vol. 2 (John Wiley and Sons, Inc., New York, 1957), pp. 167-209.

[3] J. N. Hobstetter, "Effect of Imperfections on Germanium and Silicon," Semiconductors, N. B. Hannay (ed.), (Reinhold Publishing Company, New York, 1959), pp. 508-539.

[4] J. N. Hobstetter and C. A. Renton, J. Appl. Phys. 33, 600 (1962).

electrical properties changed differently for different methods of defect introduction.

The nature of the defect introduced also depends on the type of radiation used.[5] The irradiation may consist of heavy charged particles such as protons, deuterons, alpha-particles, or bombardment by any ionized atom. The damage resulting from such charged particles is characterized by a heavy concentration of displacements along the path of the particle and a finite depth of damage determined by the range of the particle. The irradiation may consist of neutron irradiation from a source such as a reactor. Neutron irradiation tends to be more homogeneous than charged particle irradiation. The products of neutron irradiation are activated atoms due to capture of thermal neutrons with associated atomic displacement from the capture gamma recoil, and displacements due to atomic recoils from elastic collisions of the neutron with the atoms of the sample. The recoil atoms, or "knock ons," become a source of damage and behave like charged particle irradiation which is internally generated in the sample. Irradiation by electron beams tends to produce a simple defect by removing an isolated atom from its lattice site to an interstitial position leaving behind a vacancy. This interstitial-vacancy pair, or Frenkel defect, is the most simple radiation-produced defect in semiconductors and hence the defect most amenable to analysis and study. Electron irradiation has the same limitations as

---

[5] D. S. Billington and J. H. Crawford, Jr., Radiation Damage in Solids, (Princeton University Press, Princeton, 1961), pp. 11-53.

other charged particle irradiations in that the electron has a finite range in the sample, hence care must be taken to minimize the effects of non-homogeneous defect concentration.

Gamma-ray irradiation produces electron irradiation throughout the sample by means of Compton electrons.[6] The defect produced is predominantly the interstitial vacancy pair. If the energy transferred to the interstitial is insufficient to initiate a displacement cascade then such irradiation will produce a distribution of interstitials and vacancies throughout the crystal.

The changes in the electronic energy level structure of semiconductors depend strongly on the nature of the irradiation used.[7] Concepts of the nature of the introduced defect range from that of simple interstitial-vacancy pairs produced by gamma ray and electron irradiation to that of complex disordered regions resulting from energetic heavy particles.[8,9,10]

The most simple defect which might be produced in a semiconductor is the displacement of a single atom from its lattice site to an interstitial position to form an interstitial-vacancy pair. Such a defect would occur if the energy transferred per event from the incident

---

[6] O. S. Oen and D. K. Holmes, J. Appl. Phys. 30, 1289 (1959).

[7] E. I. Blount, J. Appl. Phys. 30, 1218 (1959).

[8] Billington and Crawford, op. cit., pp. 76-170, 312-368.

[9] B. R. Gossick, J. Appl. Phys. 30, 1214 (1959).

[10] J. H. Crawford, Jr. and J. W. Cleland, J. Appl. Phys. 30, 1204 (1959).

radiation were just enough to displace an atom from its normal position in the lattice. The minimum energy required to produce such a single interstitial pair has been the subject of considerable investigation.[11]

Brown and Augustyniak considered both orientation of the crystal and the temperature of the irradiation.[12] Brown and Augustyniak found that electron energies above 400 thousand electron volts (Kev) were required to produce defects in n-type germanium at 70 degrees Kelvin (^{o}K). This corresponds to a displacement energy of 16 electron volts (ev) as a threshold energy in n-type germanium. The defect production rate increased sharply as the electron energy was increased above 400 Kev.

The cross sections for the displacement of lattice atoms by gamma rays for energies up to 5 million electron volts (Mev) have been calculated by Oen and Holmes.[13] If one uses the average value of 1.3 Mev for Cobalt 60 gamma irradiation and the Z for germanium of 32, the curves of Oen and Holmes give a cross section for production of primary displacements by photo-electrons of about 5×10^{-27} centimeters^2 (cm^2). The cross section for defect production resulting from particles produced by pair production is negligibly small. Hence, the dominant process by which cobalt 60 gamma irradiation produces lattice defects is the irradiation of Compton electrons produced inside the crystal by the

---

[11] J. J. Loferski and P. Rappaport, J. Appl. Phys. 30, 1296 (1959).

[12] W. L. Brown and W. M. Augustyniak, J. Appl. Phys. 30, 1300 (1959).

[13] Oen and Holmes, loc. cit.

cobalt 60 gamma radiation. Since the electron irradiation is produced inside the crystal, the resulting defects are distributed homogeneously throughout the crystal. Since the measurements are interpreted in terms of the bulk properties of the material, the homogeneity of the sample becomes an important consideration. This is particularly important in the case of a semiconductor such as germanium in which defect gradient can produce nonlinear electrical properties. Consequently there is a definite advantage in having a homogeneous distribution of defects.

The defect configuration resulting from irradiation has been found to be dependent upon the temperature at which the irradiation is conducted as well as on the type of radiation used.[14] MacKay and Klontz found that n-type germanium irradiated at about $10^{\circ}K$ by 1.1 Mev electrons showed a pronounced annealing which occurred in two stages; one at $34^{\circ}K$ and another at $64^{\circ}K$. They estimate the activation energies to be approximately 0.04 ev and 0.07 ev respectively. Since the activation energy for vacancy motion is estimated to be of the order of 1 ev,[15] the process observed by MacKay and Klontz is probably not vacancy diffusion. Further investigation by MacKay and Klontz has shown that the relative amount of annealing in each of these temperature ranges depends upon the total flux which the sample receives. No appreciable annealing occurs in the $35^{\circ}K$ stage for fluxes less than 10^{16} electrons/cm^2. About half the

---

[14] J. W. MacKay and E. E. Klontz, J. Appl. Phys. 30, 1269 (1959).

[15] H. Letaw, Jr., L. M. Slifkin, and W. W. Portnoy, Phys. Rev. 93, 892 (1954).

recovery is in each stage for fluxes above 10^{17} electrons/cm^2.[16,17] The per cent of annealing in the 64°K stage varies with bombardment energy from 10 per cent for 600 Kev electrons to 50 per cent for 1.0 Mev.

These authors interpret this annealing as resulting from the recombination of the nearest and next nearest stable interstitial-vacancy pairs. The work of MacKay and Klontz clearly shows that the defect configuration at 10°K and 78°K must differ. One might also suspect that irradiation at 10°K, 78°K, and room temperature might lead to different defect configurations.

One can therefore conclude that the defect structure resulting from irradiation depends upon:

1. The type of radiation used;
2. The total dose received by the sample;
3. The temperature at which the irradiation was conducted; and
4. The energy of the irradiation used.

The annealing of the irradiation induced changes in the electrical properties has been used for some time as a means of studying both the nature of irradiation induced defects and their energies of motion. A series of experiments was conducted by Brown, Fletcher, and Wright using 3 Mev electrons to irradiate n-type germanium.[18] The irradiations were

---

[16] E. E. Klontz and J. W. MacKay, Bull. Amer. Phys. Soc., Series II, 6, 303 (1961).

[17] J. W. MacKay and E. E. Klontz, Symposium on Radiation Damage in Solids and Reactor Materials, Venice, Italy, May 1962, To be published.

[18] W. L. Brown, R. C. Fletcher, and K. A. Wright, Phys. Rev. 92, 591 (1953).

conducted at room temperature. They obtained an activation energy of 1.7 ev for the annealing of the induced defects which they interpreted to be vacancies. They estimated that the defects produced by 3 Mev electrons would be isolated interstitial-vacancy pairs.

More recent work by Brown, Augustyniak, and Waite has shown the annealing process to be more complicated than had been previously assumed.[19] The work of Brown and co-workers indicated the annealing of the radiation induced changes in electrical properties such as the conductivity and carrier concentration to be a strong function of the impurity type and concentration. A similar result was obtained by Curtis in the annealing of irradiation induced changes in the minority carrier lifetime.[20]

The purpose of this study was to investigate the annealing behavior of antimony doped n-type germanium under carefully controlled conditions in an attempt to learn some of the details of the processes involved in such annealing which occurs in the range of 78°K to 455°K. The type of irradiation, sample impurity, and temperature of irradiation were the same for all samples studied. The irradiations were all performed in the same source. All irradiations were conducted with the sample immersed in liquid nitrogen. Similarity of samples was obtained by taking all samples from the same ingot.

---

[19] W. L. Brown, W. M. Augustyniak, and J. R. Waite, J. Appl. Phys. 30, 1258 (1959).

[20] O. L. Curtis and J. H. Crawford, Jr., Phys. Rev. 126, 1342 (1962).

The annealing temperature and annealing times were the controlled variables, the annealing kinetics and activation energies involved were studied using these variables.

CHAPTER II

EXPERIMENTAL PROCEDURE

A. Measurement of Changes in Carrier Concentration

The free carrier concentration as measured by the Hall-effect is a convenient quantity by which to study changes in semiconductors. When the sample is in the extrinsic condition, the sign of the Hall voltage indicates the type of carrier. The magnitude of the Hall voltage is a measure of the free carrier concentration.[1] Since the free carrier concentration is the algebraic sum of the concentration of the various charge centers multiplied by their respective ionization state, the carrier concentration is a measure of the ionized charge center concentration. Consequently, a measurement of the carrier concentration can also be a direct measurement of the concentration of crystal defects.

The Hall coefficient, R, is related to the carrier concentration for intrinsic material by the relation

$$R = \frac{3\pi}{8e} \frac{p\,\mu_h^2 - n\,\mu_e^2}{(p\,\mu_h + n\,\mu_e)^2} \qquad \text{electromagnetic units (emu)} \qquad (1)$$

where n is the electron concentration,

p is the hole concentration,

μ_e is the electron mobility,

μ_h is the hole mobility, and

---

[1] W. E. Shockley, Electrons and Holes in Semiconductors. (D. Van Nostrand and Company, New York, 1950), pp. 204-217.

e is the electronic charge.

At thermal equilibrium, n and p are related by the expression[2]

$$np = 4 \left(\frac{2\pi\, \bar{m}^* kT}{h^2}\right)^3 e^{-E_g/kT} \quad \text{centimeters}^{-6}, \; (\text{cm}^{-6}) \qquad (2)$$

where E_g is the energy width of the forbidden band

$\bar{m}^*$ is the geometric mean of the effective masses of the electrons and holes,

h is Plank's constant,

k is the Boltzman constant, and

T is the temperature (^{o}K).

The coefficient in equation 2 is a product of a constant and the cube of the temperature. For germanium this expression becomes

$$np = 2.33 \times 10^{31}\, T^3\, e^{-E_g/kT} \quad (\text{cm}^{-6}).$$

If electron donor impurities are present in the crystal to such an extent that

$$n \gg p,$$

then the sample conductivity is said to be n-type, and the sample is in the extrinsic condition. Conversely when $p \gg n$ the sample is said to be p-type.

For a sample in the extrinsic condition

$$R = (\pm) \frac{3\pi}{8e\, n_i},$$

where n_i refers to the concentration of the excess carriers and the sign

---

[2] Ibid., p. 245.

is + for p-type and - for n-type.

The concentration of excess carriers is thus given by

$$n_i = \frac{7.38 \times 10^{18}}{R} \qquad cm^{-3}.$$

The Hall coefficient is given by[3]

$$R = \frac{V\ t}{I\ H} \times 10^8 \qquad cm^3\ coulomb^{-1},$$

where V is the Hall voltage in volts,

t is the thickness of the sample,

I is the current in amperes,

H is the magnetic field in gauss, and

H is perpendicular to I.

Consequently one can measure the type and magnitude of the charge carrier concentration in terms of a length, current, magnetic field, and a voltage. Changes in charge carrier concentration will then be observed as a change in voltage to current ratio.

The experimental procedure used in the study reported here was as follows:

1. The Hall coefficients of samples of n-type germanium single crystals were measured as a function of temperature from 77°K up to well into the intrinsic range before irradiation.

2. The samples were then exposed to cobalt 60 gamma irradiation at 77°K until approximately 90 per cent of the conduction electrons had been removed. The intensity of the cobalt 60 source was 5×10^6

---

[3] W. Crawford Dunlap, Jr., An Introduction to Semiconductors, (John Wiley and Sons, Inc., New York, 1957), p. 6.

Roentgen per hour (R per hr.). Some of the samples were monitored during the irradiation in order to determine the carrier removal rates.

3. Subsequent to irradiation, some of the samples were given isochronal anneals to survey the annealing behavior and to establish the proper temperatures for isothermal annealing. The sample temperature was brought to an annealing temperature which was maintained for 20 minutes. The temperature was then reduced to the reference temperature of 77°K for measurement. After measurement the sample temperature was brought to a higher annealing temperature and held for 20 minutes. This process was repeated at successively higher temperatures until the temperature ranges of the various steps of annealing had been determined.

4. The Hall constant as a function of temperature for those samples which were to be isothermally annealed was measured within the temperature limits which were established by the isochronal anneals as the temperature range in which annealing was not measurable.

5. Subsequent to irradiation, some of the samples were subjected to isothermal anneal at pre-determined temperatures.

6. Before and after each annealing period, the temperature was lowered to a reference temperature at which the Hall constant was measured. The reference temperatures used were 77°K and 273°K.

7. The data was then plotted in terms of a normalized fraction of induced carrier concentration change remaining. This parameter was designated f(n).

The parameter f(n) was computed from the relationship

$$f(n) = \frac{n_o - n_t}{n_o - n_r},$$

where n_o = the carrier concentration before irradiation,

n_r = the carrier concentration after irradiation, and

n_t = the carrier concentration after anneal.

The values of f(n) ranged from 1 immediately after irradiation to 0 when all the induced change had been removed.

B. Measurement in Changes of Reciprocal Mobility

The conductivity (σ) for n-type extrinsic material is given by

$$\sigma = n\, e\, \mu ,$$

where n is the conduction electron concentration,

e is the charge of the electron, and

μ is the electron mobility.[4]

Using laboratory units of gram, cm, sec, volts, coulombs, and gauss, the Hall constant becomes

$$R = \frac{3\pi}{8} \frac{1}{n(\pm e)} .$$

Hence the mobility is given by

$$\mu = \frac{8}{3\pi} R\sigma = \frac{8}{3\pi} \frac{R}{\rho} ,$$

where ρ is the resistivity.

The mobility is related to the mean free time the electron travels between scattering collisions by

$$\mu = \frac{e}{m} \tau .$$

where τ is the mean free time between scattering collisions. The mean

---

[4] W. Shockley, Electrons and Holes in Semiconductors, (D. Van Nostrand Company, Inc., New York, 1950), pp. 187-217.

free time is proportional to the product of the thermal velocity of the electron ($\bar{v}$) and the mean free path l,

$$\tau = \bar{v}\, l \quad .$$

Since the mobility depends upon the thermal velocity of the electrons, the mobility is temperature dependent. For lattice scattering, the mobility is approximately proportional to the minus three halves power of the temperature.[5] For germanium, this lattice contribution to the mobility μ_L is given by

$$\mu_L = 19 \times 10^6\, T^{-3/2} \quad .$$

The scattering by ionized centers is coulomb scattering. The mobility (μ_I) resulting when coulomb scattering is the scattering mechanism has been calculated by Conwell. The expression for germanium is

$$\mu_I = 8.5 \times 10^{17} \left(\frac{m}{m_{eff}}\right)^{1/2} \frac{T^{3/2}}{N_I \ln\left(1 + 8.3 \times 10^8 \frac{T^2}{N_I^{2/3}}\right)}$$

where N_I is the concentration of charge centers, and

m_{eff} is the effective mass of the electron.

The Conwell expression gives the reciprocal mobility to be proportional to the concentration of the scattering charge centers. One may choose m_{eff} to be $m/4$.[6] Using this value, one obtains for the reciprocal mobility for germanium

$$\frac{1}{\mu} = 5.93 \times 10^{-19}\, T^{-3/2}\, N_i \ln\left(1 + 8.3 \times 10^8 \frac{T^2}{N_i^{2/3}}\right) \quad .$$

---

[5] E. M. Conwell, Proc. IRE 40, 1327 (1952).

[6] P. P. Debye and E. M. Conwell, Phys. Rev. 93, 693 (1954).

Since N_i may not be identical with the change in carrier concentration, it is necessary to study the change in mobility during the annealing process.

A function $f(\frac{1}{\mu})$ may be defined by

$$f(\frac{1}{\mu}) = \frac{\frac{1}{\mu_o} - \frac{1}{\mu_t}}{\frac{1}{\mu_o} - \frac{1}{\mu_r}} ,$$

where μ_o is the pre-irradiation mobility,

μ_r is the post-irradiation mobility, and

μ_t is the mobility measured after anneal.

C. Sample Preparation

The samples were made by slicing disks perpendicular to the growth axis of the crystal and cutting samples from the disk by means of an ultrasonic cutting die. The configuration of the resulting sample is shown in Figure 1. The surface of the sample was then etched with CP4 etch and washed with 95 per cent ethyl alcohol.[7] Typical sample dimensions are:

$t = 0.075$ cm,

$w = 0.20$ cm, and

$l = 0.50$ cm.

Electrical connection was made to the sample by soldering #36

---

[7] CP4 etch consists of twenty parts concentrated nitric acid, twelve parts 50 per cent hydrofluoric acid, twelve parts glacial acetic acid, and one-half part bromine.

UNCLASSIFIED
ORNL-LR-DWG 72836

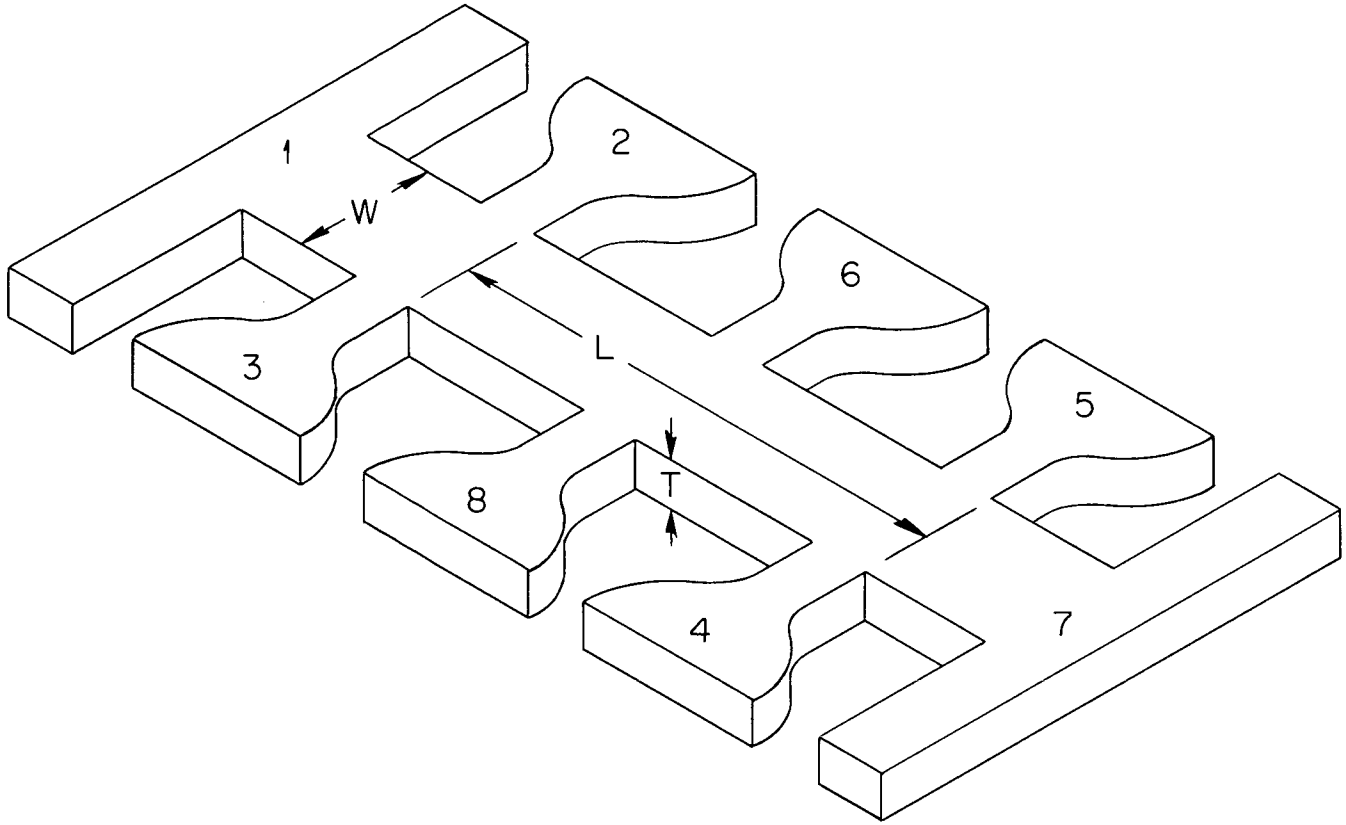

Figure 1. Sample configuration.

wire to the ends and large surfaces of the projecting sections using a lead-tin solder containing 2 per cent antimony. Zinc chloride solution was used as a flux. The resulting contacts were checked for rectification both with the sample at room temperature and with the sample immersed in liquid nitrogen.

Those contacts which rectified sufficiently to be detected with a resistance measurement using a Simpson Multimeter were re-etched and re-soldered. Only samples with non-rectifying contacts were used.

Rectifying contacts cause minority carrier injection and general non-ohmic behavior which would yield spurious values for the properties measured.[8]

D. Sample Homogeneity

The influence of carrier concentration gradients on the galvanomagnetic effects in semiconductors has been investigated by Bate and Beer.[9] Bate and Beer were primarily interested in the effect of conductivity gradient on magneto resistance, however, their work shows that a conductivity gradient can produce an electric field component parallel to the Hall field. Consequently the Hall constant measured in such a sample would not give a true measurement of the carrier concentration. This spurious voltage would change during an irradiation and annealing experiment resulting in an erroneous behavior of f(n). A

---

[8] George C. Haiman and Theodore Higier, J. Appl. Phys. 33, 2198 (1962).

[9] R. J. Bate and A. E. Beer, J. Appl. Phys. 32, 806 (1961).

sample having a 1 per cent gradient before irradiation would have a 10 per cent gradient after the irradiation had removed 90 per cent of the carriers.

A carrier gradient in any direction will produce an erroneous value for the conductivity. Since this will vary with temperature, the temperature characteristic of the mobility can be altered considerably by such gradients.

A gradient in carrier concentration can also be produced by a gradient in the irradiation field. A uniform sample irradiated in a gamma field which was 1 per cent more intense at one end of the sample than at the other end would produce a 10 per cent gradient in the carrier concentration after irradiation. Consequently it was necessary to take every practical precaution to assure that the sample was homogeneous and that carrier concentration gradients were not produced during the irradiation.

Each sample was checked for gradients in the carrier concentration. Terminals 1 and 7 were used as current connections. Terminals 6 and 8 were used as Hall voltage connections. Acceptable samples showed zero voltage across terminals 6 and 8 for both directions of current when the sample was out of the magnetic field. The magnitude of the Hall voltage was the same for either direction of current flow when the sample was in the magnetic field. As a further check, a 100K 10 turn Helipot was connected across terminals 3 and 4. The Helipot was then adjusted so that the voltage between the sliding contact and contact 6 was zero when the sample was out of the magnet. A zero setting of less than 5 per

cent deviation from the center point was accepted providing the setting did not change when the current in the sample was reversed. This latter check was sensitive not only to the gradient of carrier concentration between contacts 4 and 3 but also was indicative of the presence of carriers injected by the current contacts.

These checks were made before and after irradiation.

E. Sample Holder

The sample was placed in the holder as is shown in Figure 2. Electrical insulation between the sample and the phosphor bronze was provided by a layer of cellulose acetate tape placed on the phosphor bronze strip. Electrical isolation was thus provided without undue thermal insulation.

The slot in the sample stick protects the sample against breakage. The phosphor bronze strip is secured by wrapping the entire assembly with cellulose acetate tape. The sample is then in an enclosed chamber. Thus when the sample is transferred from the irradiation facility to a handling or measuring facility the transfer can be made without completely removing the sample from a liquid nitrogen bath.

This technique for maintaining the sample at liquid nitrogen temperature made it possible to conduct the exploratory isochronal anneals starting at 77°K.

F. Annealing Procedure

During measurement the sample was placed in a furnace in which a temperature can be maintained in the range from liquid nitrogen up to

UNCLASSIFIED
ORNL-LR-DWG 72837

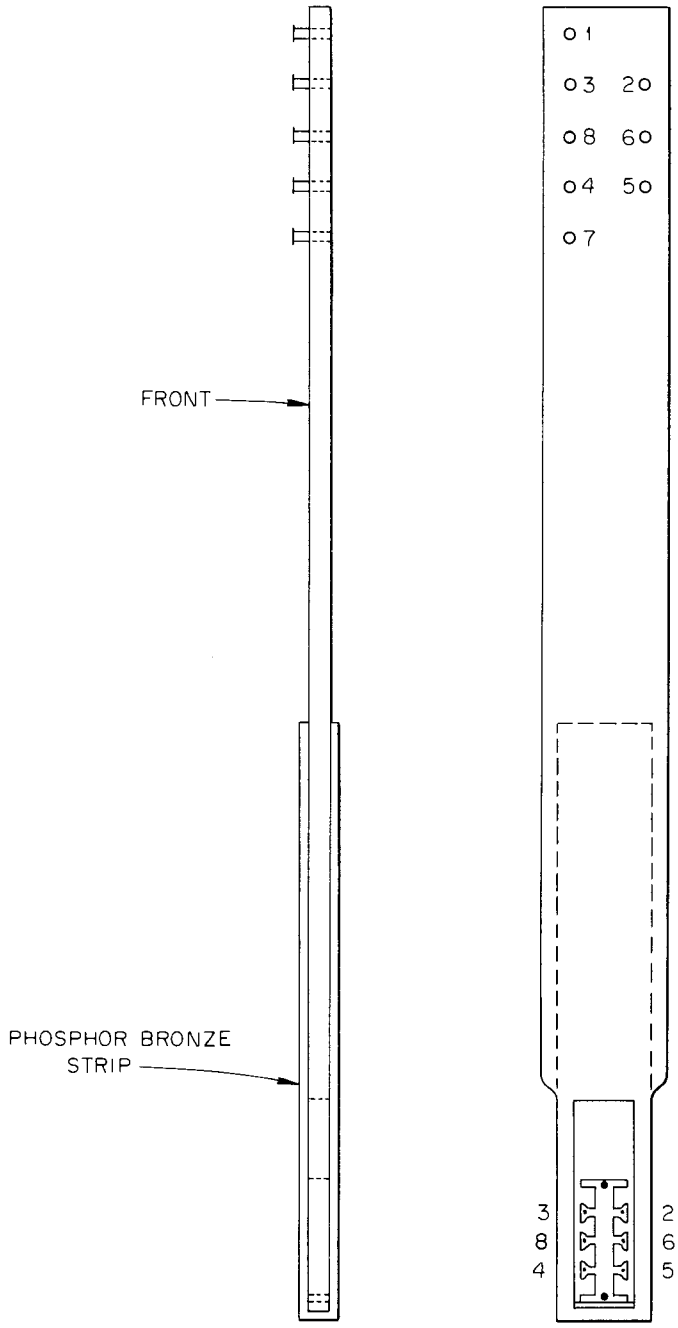

Figure 2. Sample holder.

about 200°C. The arrangement is shown schematically in Figure 3. The sample holder was held against one side of the sample chamber by means of a phosphor bronze spring. The thermocouple used both for temperature measurement and control was imbedded in the copper sample chamber directly behind the sample. The heat sink for the system was provided by a copper rod which connects the sample chamber to a liquid nitrogen bath. Temperature equilibrium of the sample was monitored after a temperature change by recording the sample resistivity. Thermal equilibrium was inferred when the resistivity change had stabilized at a new value. In practice this required a waiting time of about ten minutes after a temperature change.

It was observed during initial testing of the equipment that because of thermal lag in the assembly, a small amount of over-shoot in the temperature of the furnace would result in a sharper temperature pulse in the sample as observed from the resistivity changes. By this means, the uncertainty in the leading edge of the temperature pulse in the sample was reduced to less than three minutes. Since the isochronal anneals were twenty minutes long, the isochronal anneals were conducted using the temperature control furnace in the measuring apparatus.

Some isothermal anneals which were conducted at low temperature required times long compared to three minutes before significant changes were observed. Consequently some samples were annealed isothermally without being removed from the temperature control furnace.

The majority of the isothermal anneals were conducted by plunging the sample into a silicone oil bath which was maintained at the annealing

UNCLASSIFIED
ORNL-LR-DWG 72838

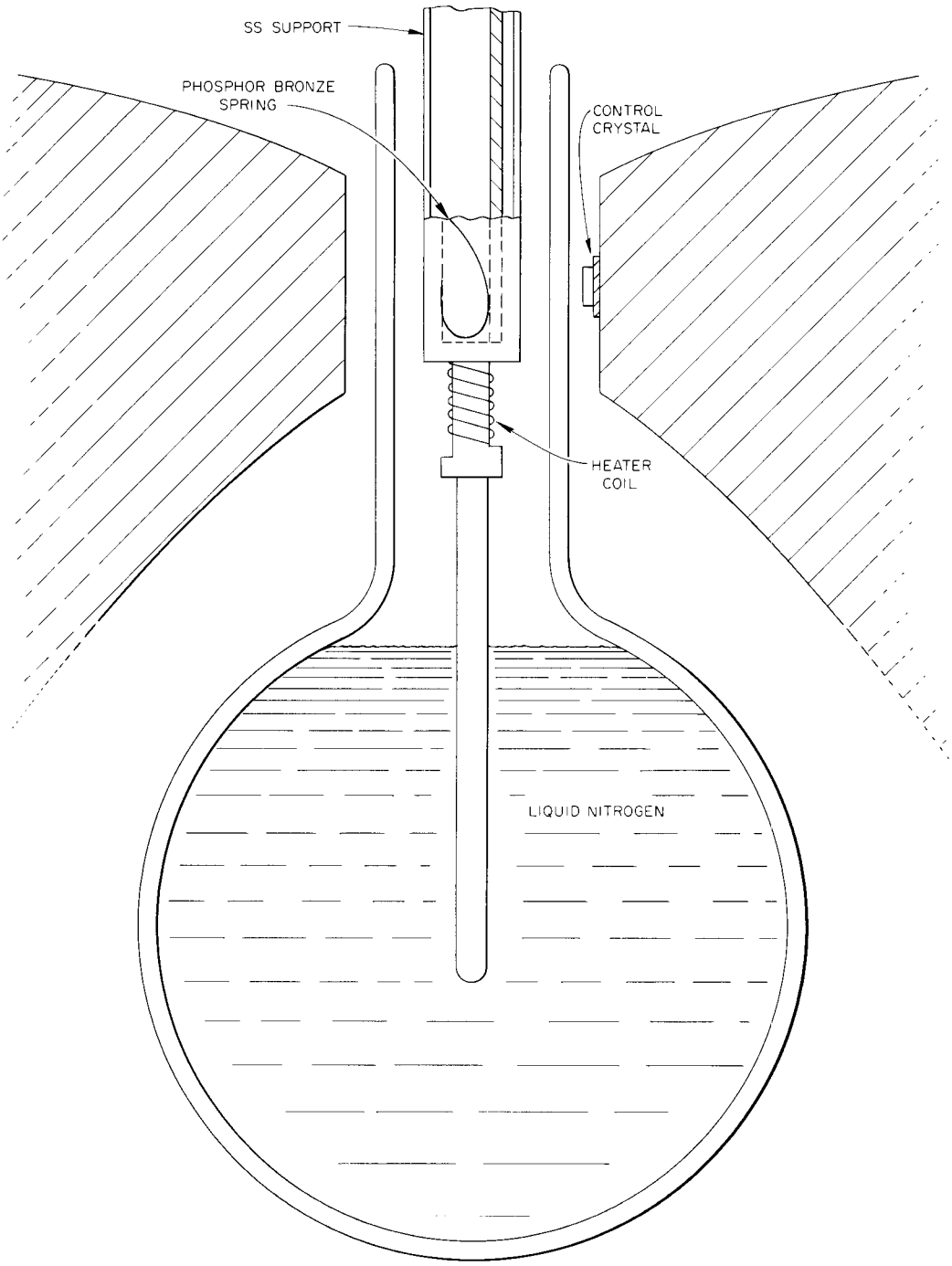

Figure 3. Schematic of temperature control furnace in measuring position.

temperature. The thermal shock resulting from plunging the sample into the hot oil resulted several times in separation of contacts from the sample. Since the anneals were conducted at temperatures above 273°K, it was possible to resolder the contacts while the body of the sample was immersed in a distilled water-ice slurry. Such resoldering did not anneal the sample and usually produced acceptable contacts. When acceptable contacts could not be made, the anneal was terminated and the experiment repeated with a new sample.

G. The Magnetic Field

The magnetic field was produced by an electro-magnet. The magnetic field was controlled at 5000 gauss by controlling the current through a resistance in series with the magnet coil. The voltage developed across the resistor was compared with a stable pre-set demand voltage. The difference signal was used as the input to a servo amplifier which controlled the current in the field coil of a dc generator. The dc generator served as the power supply for the magnet.

The magnetic field was measured using a rotating coil gaussmeter which had been calibrated by comparison with a field measured by proton resonance. The magnetic field was reproducible to within 1 per cent over a test of several days during which the field had been cycled from 5000 gauss to zero many times.

Measurement of the resistivity of the sample required a zero magnetic field. The magnet was controlled at zero gauss by adjusting the current in the magnet until a germanium plate fastened to the pole

face showed zero Hall voltage. The control circuit was capable of reversing the current in the magnet. Without this provision for zero field, the resistivity measurements would include a contribution from the magneto resistance produced by the residual flux in the magnet. Thus the resistivity measurements would be in error. The magnitude of the residual flux would not be constant, since it would depend upon the time elapsed since the current in the magnet coils had been turned off. Consequently, the resistance readings would be scattered as well as in error.

H. The Measuring Circuit

The measuring circuit is shown schematically in Figure 4.

The measurements were made using a null technique in which the current through the sample entered into the measurements in such a way as to cancel. The resultant measurement was made by an analogue computing circuit which operated on a shared time basis between Hall and resistivity. The output was recorded on a twelve point recorder. The circuit is shown schematically in Figure 4.

Switch 3 in Figure 4 is shown in the resistivity position. When the chopper (sw 2) is connected across C_1, a current will flow in the transformer primary if the voltage on C_1 is different than that on C_3. When the chopper is connected across C_2, a current will flow if the voltage across C_2 is different than that across C_3. These pulsating currents produce a signal which can be amplified and cause the servo motor to adjust R_4 until the voltage across C_1 and C_2 are equal. At this null position there is no current drawn from the sample.

UNCLASSIFIED
ORNL-LR-DWG 72839

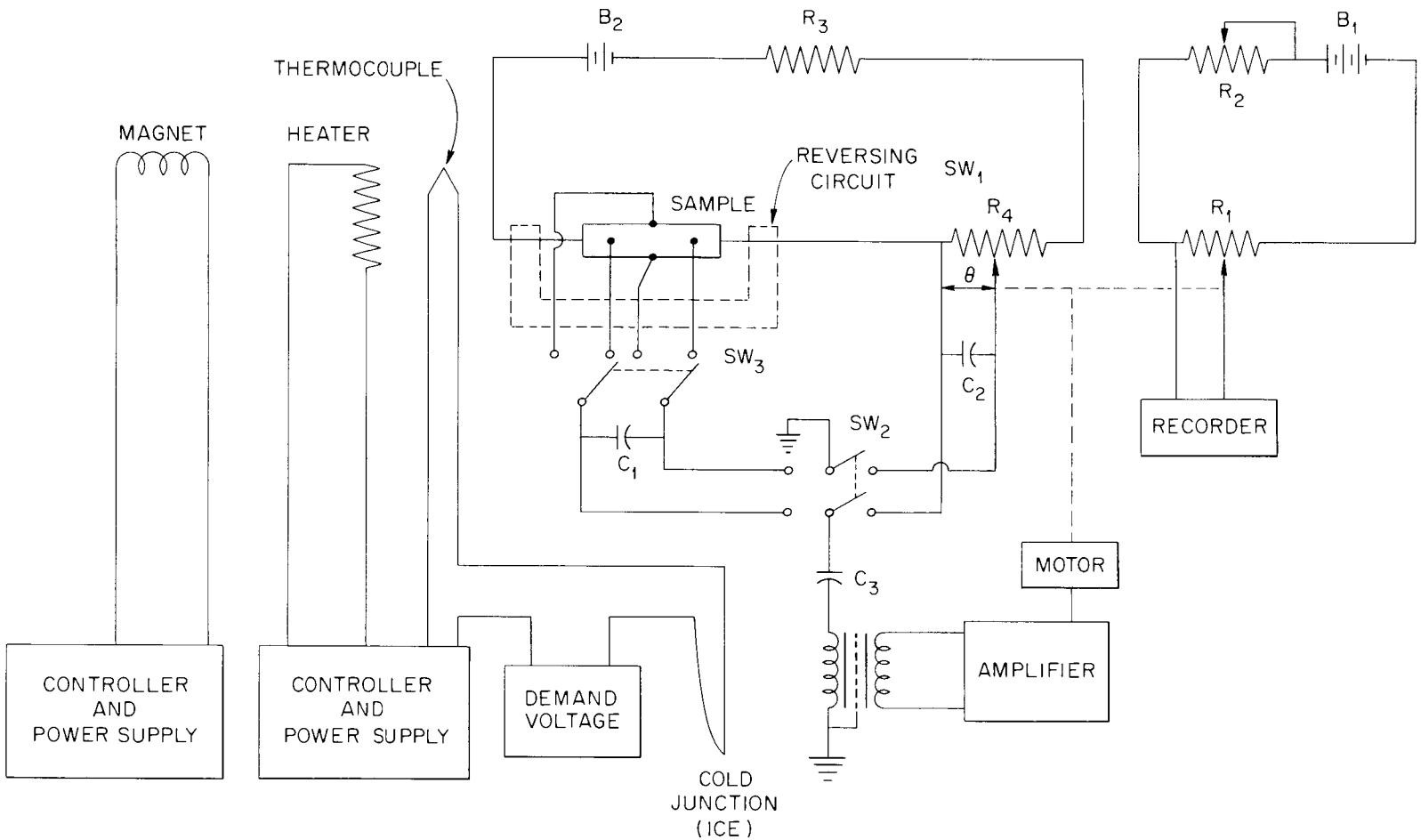

Figure 4. Measuring circuit schematic.

In addition to providing a null type measurement, this technique allows four terminal measurements with complete isolation between the two pairs of terminals. Consequently there is no dc interaction between the various parts of the circuit as a result of making the measurement.

The voltage between the resistivity contacts is given by

$$V_s = \rho \frac{l}{t\,W} I ,$$

where ρ is the bulk resistivity,

l is the distance between the contacts,

t is the sample thickness,

W is the sample width, and

I is the current.

The voltage across C_2 is given by

$$V_R = r\,\theta\,I,$$

where r is the resistance per unit displacement,

θ is the displacement, and

I is the current.

At balance,

$$\rho \frac{l}{t\,W} I = r\,\theta\,I,$$

$$\rho = \frac{t\,W}{l} r\,\theta .$$

Hence the resistivity is given in terms of the product of two constants and the position of the resistor contact. One constant is determined by the dimensions of the sample. The second constant is determined by the resistance of the resistor. These two constants are known.

The sliding contact of R_1 is mechanically connected to the sliding

contact of R_4. B_1 is a constant voltage supply. The current is adjusted by R_2 until the recorder reads full scale for the maximum value of R_1.

The resistivity is then given by the recorder reading times the sample constant times the magnitude of R_4. The magnitude of R_4 is also recorded. The Hall coefficient is given by

$$R = \frac{E_H}{J\,H},$$

where R is the Hall coefficient,

E_H is the electric field produced by the Hall effect,

J is the current density, and

H is the magnetic field. Since

$J = \frac{I}{t\,W}$, then R is given by

$$R = \frac{E_H\,t\,W}{I\,H} = \frac{V\,t}{I\,H},$$

where V is the voltage produced across the sample.

If one expresses

V in volts,

t in cm,

I in amperes, and

H in gauss,

the expression becomes

$$R = \frac{V\,t}{I\,H} \times 10^8 .$$

The voltage V can thus be expressed as

$$V = \frac{R\,I\,H}{t} \times 10^8 = r\,\theta\,I .$$

Hence R is given by

$$R = \frac{r\ \theta\ t}{H} \times 10^8 \ .$$

The Hall constant is thus expressed in terms of the scale factor, r, a known constant, and the position of the sliding contact.

CHAPTER III

EXPERIMENTAL RESULTS

A. Isochronal Survey of Carrier Concentration Annealing

A survey of the effective temperature range for annealing was made by means of an isochronal anneal using successive temperature pulses of twenty minutes duration starting at $77^{\circ}K$ and increasing to $425^{\circ}K$ in $5^{\circ}K$ increments.

An isochronal anneal of one sample on warmup after gamma irradiation is shown in Figure 5. These data are in qualitative agreement with that of Brown, et al.,[1] taken on annealing of damage introduced by 0.5 Mev electron irradiation (Figure 6). The carrier concentration of the material used by Brown, et al., was of the order of 3×10^{14} cm^{-3}. The carrier concentration of the material used here is of the order of 10^{14} cm^{-3}.

In both Figure 5 and Figure 6 there is an increase in the induced carrier change in the temperature range below $300^{\circ}K$. Brown attributes this increase to the emptying of minority carrier traps. This interpretation is in agreement with the observations of Haynes and Hornbeck, and Shulman.[2,3] An increase in conductivity was observed due to

---

[1] W. L. Brown, W. M. Augustyniak, and T. R. Waite, J. Appl. Phys. 30, 1258 (1959).

[2] J. R. Haynes and J. A. Hornbeck, Phys. Rev. 90, 152 (1953).

[3] R. G. Shulman, Phys. Rev. 102, 1451 (1956).

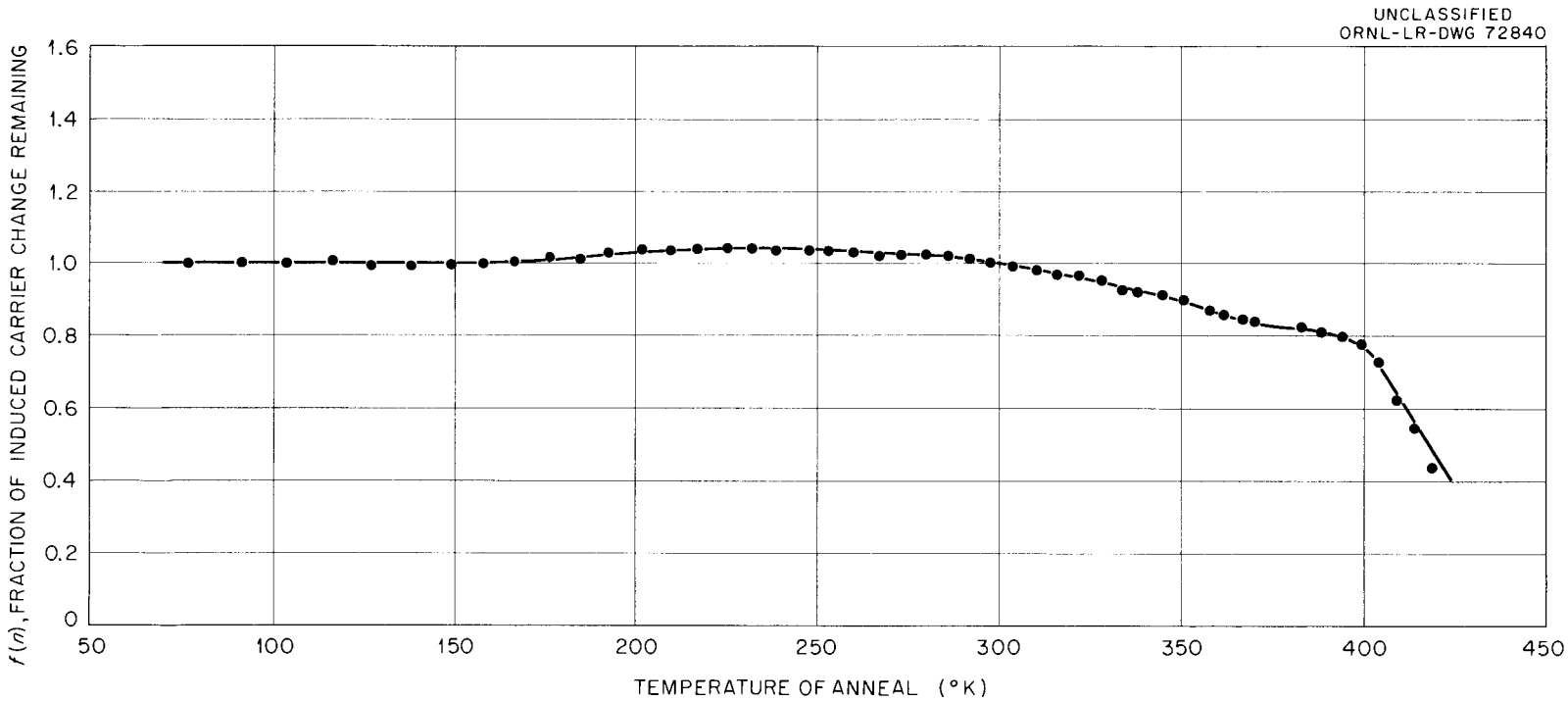

Figure 5. Isochronal anneal EP8-A.

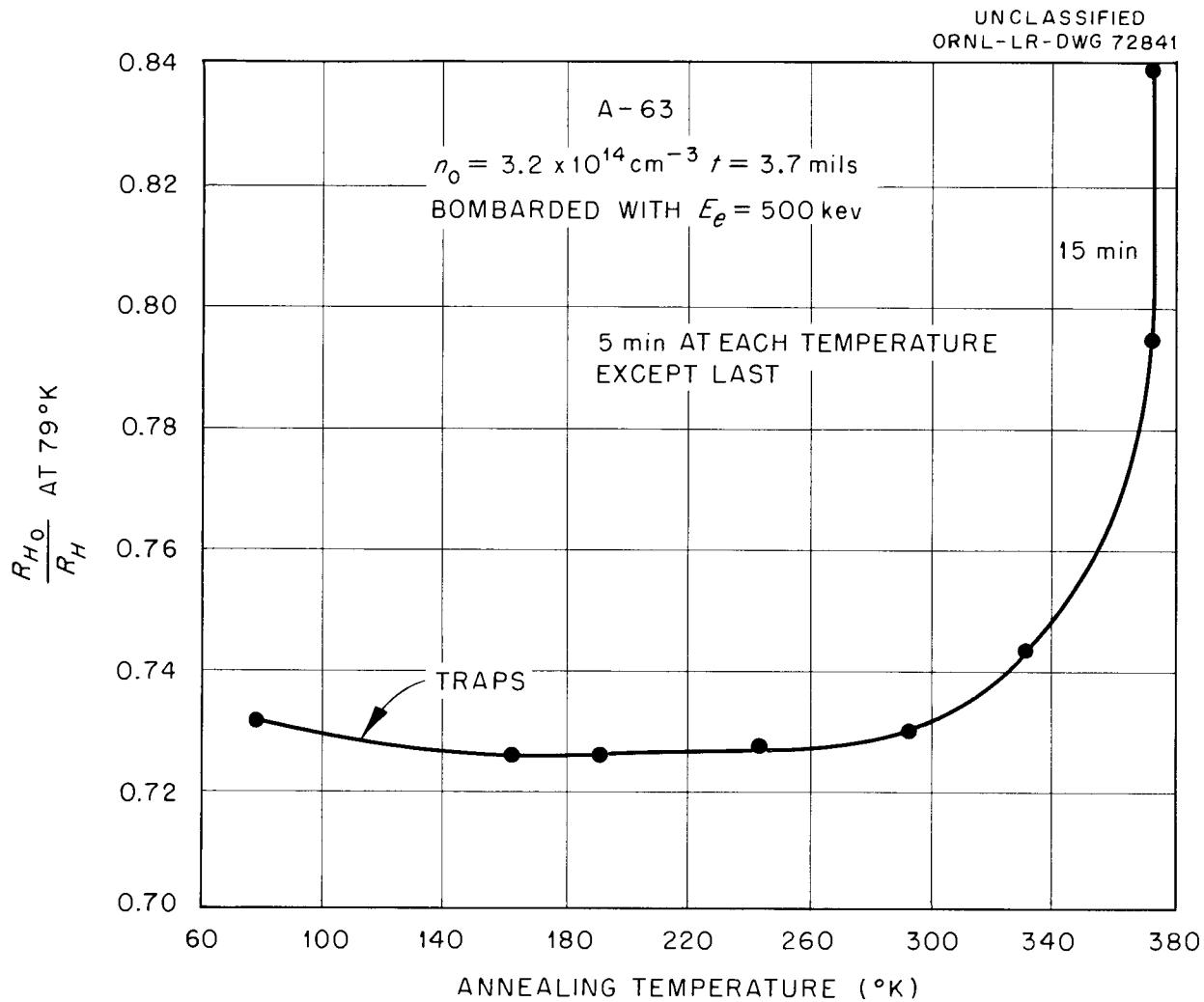

Figure 6. Isochronal anneal data of Brown, Augustyniak, and Waite.

photo excitation of holes to these trapping centers leaving in the conductivity band a corresponding concentration of excess electrons. These trapping centers are effective at temperatures below 183°K. Schulman observed the introduction of such minority carrier trapping centers in germanium by high energy electron bombardment.[4]

Since the samples in this experiment were annealed in the dark, it was not possible to differentiate between annealing and release of minority carriers from traps. The release of trapped minority carriers would result in a permanent change since there was no light present to re-excite minority carriers to the traps when the sample was measured at 77°K after the temperature pulse. The evidence of previous work, however, strongly supports Brown's explanation.

A second sample was exposed and given an isochronal anneal to study the details of the annealing structure in the region above 273°K. These data are shown in Figure 7. Comparison of the two isochronal anneals shows the same general behavior for the 77°K readings. EP8-A was found to have a carrier gradient which accounts for the small discrepancies in the details of the 77°K curve. The effect of the gradient is to smear out the drop in the curve at 320°K. The general shape and the points at which the different annealing processes begin were the same in the two curves.

The critical temperatures were also the same here as those in the sample of Brown, et al., which had approximately twice as large a carrier

---

[4] Ibid.

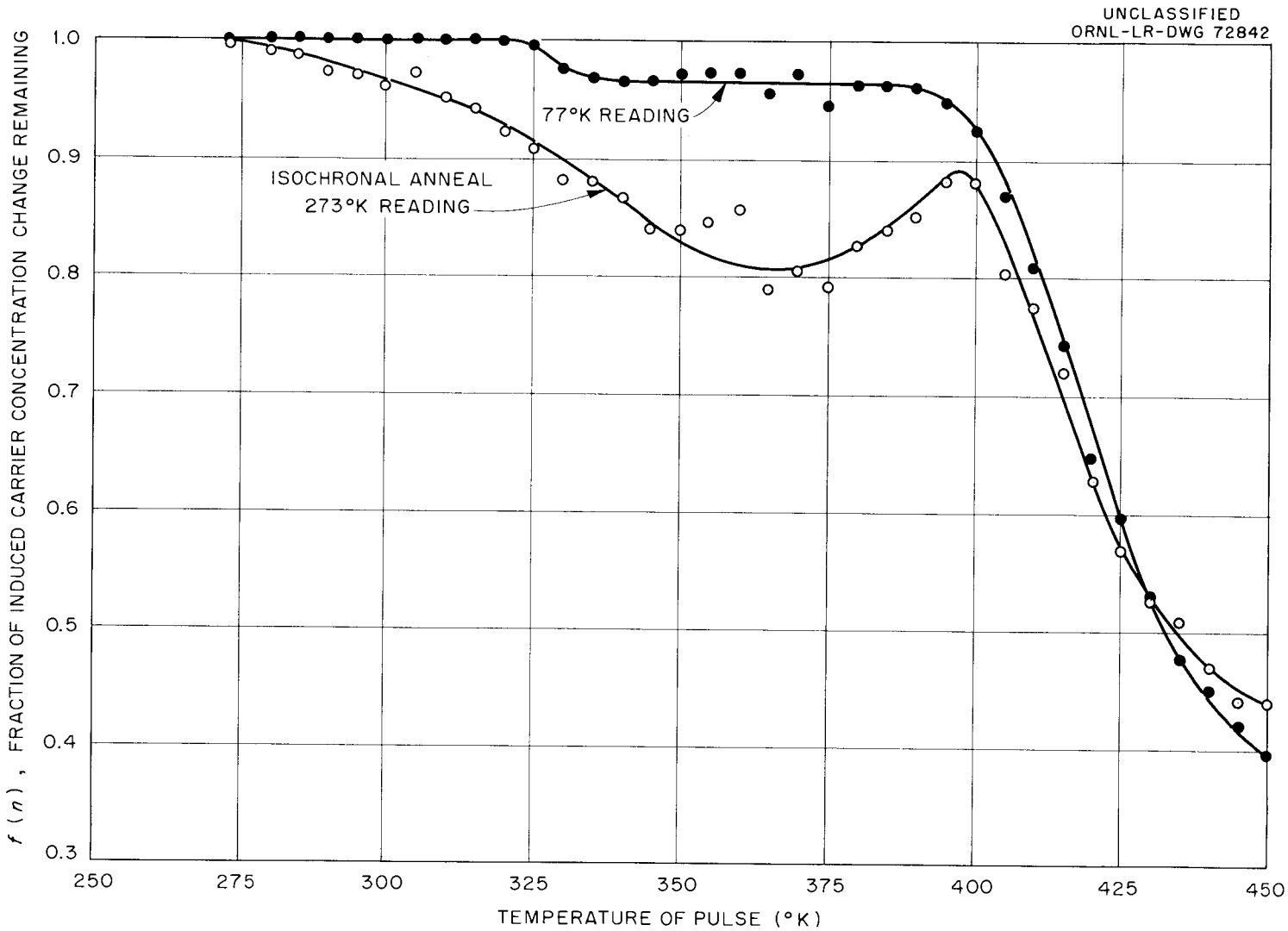

Figure 7. Isochronal anneal of EP8-K.

concentration.

The most obvious thing suggested by Figure 7 is the presence of more than one annealing mechanism. The region between 273°K and 320°K is characterized by annealing in the 0.2 ev level, but shows no change in the carrier concentration at 77°K. Both the 77°K and 273°K readings changed rapidly between 320°K and 340°K. From 340°K to 390°K, there was little change in the 77°K reading but there was a minimum in the 273°K readings. From 400°K up, both the deep and shallow levels were removed at about the same rate.

B. Isothermal Anneal of Carrier Concentration

A series of samples were irradiated and then annealed isothermally at temperatures in the range between 370°K and 455°K. The temperature limits were imposed by the time required to complete the anneal. The changes at temperatures above 455°K occurred too fast to allow accurate measurement of the annealing time. Temperatures below 370°K required times for annealing that were prohibitively long.

A compilation of the 77°K measurements is given in Figure 8. In every case there was a rapid annealing which removed approximately 10 per cent of the induced carrier change. There was then a period in which there was little change followed by a change which saturated and remained constant. The major anneal occurred at longer times for lower temperatures. It can also be seen that the saturation plateau was higher for lower temperatures.

After completion of the anneal of sample P at 377.2°K, the temperature of the oil bath was increased to 455°K and a second anneal was

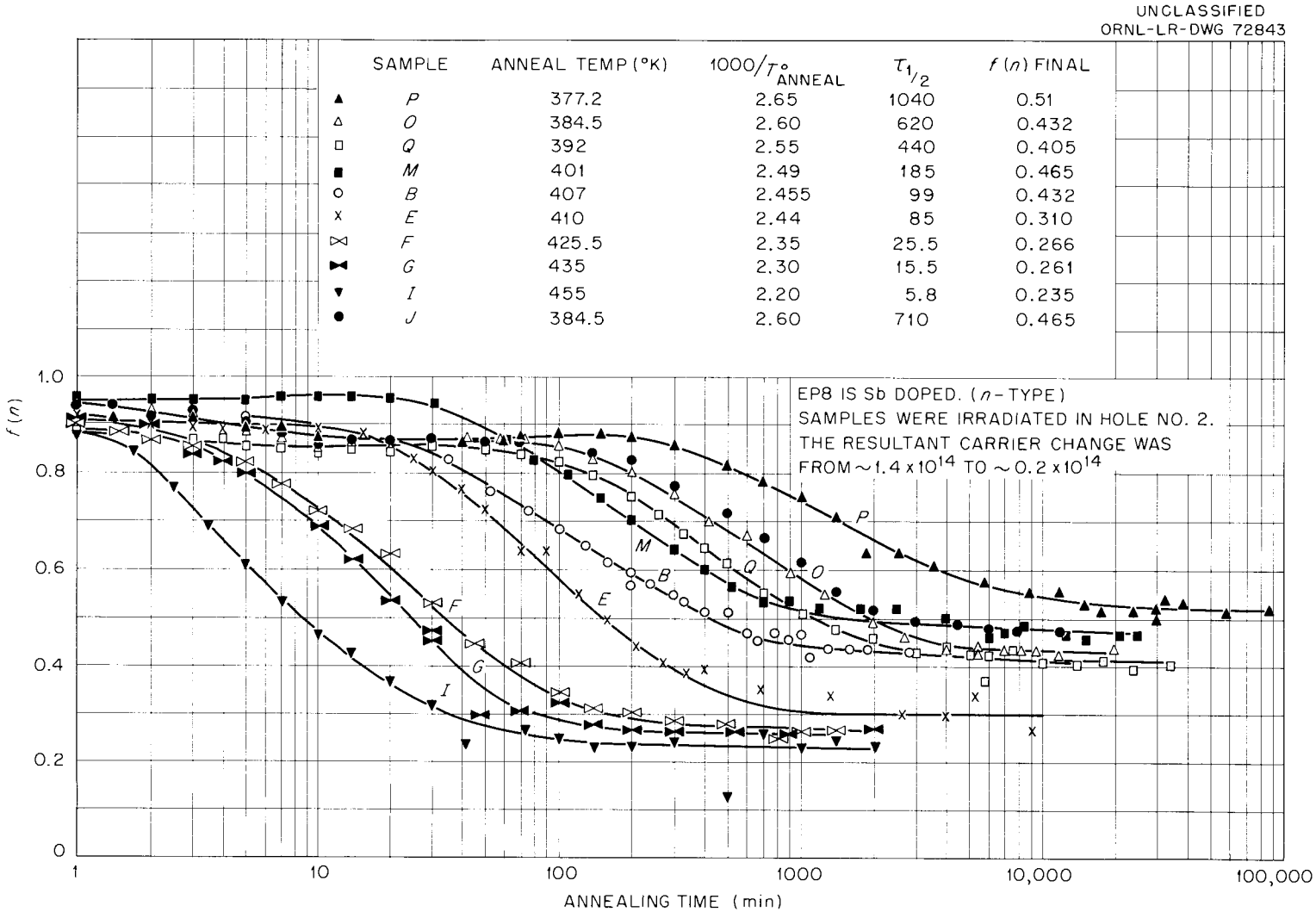

Figure 8. Summary of isothermal annealing curves measured at 77°K.

attempted at this temperature. It was expected that the saturation plateau would move from the value attained with an anneal of 377.2°K to a value characteristic of a 455°K anneal such as was observed for sample I. Comparison of the curve for sample P with that for sample I which was annealed at 455°K indicates that a change in the saturation plateau might have been expected. There was no change, however, in the plateau value of f(n) after cumulative heating for six hours.

Sample O was also heated to 455°K for several hours. The saturation plateau of this sample also remained unchanged. One may conclude, therefore, that the arrangement of defects produced by annealing is a function of the annealing temperature and once produced it is a stable arrangement for the temperature range studied.

Brown, et al., evaluated the activation energy for their curves by plotting the time required for the measured property to anneal to one half of the initial value.[5] The technique used here is to plot the time for the major annealing process to go half way to completion. This is the time required to fall half way from the initial plateau to the saturation plateau. This time has been designated $\tau_{\frac{1}{2}}$.

The insulation of the lead wires of sample M was destroyed by the irradiation. This required that the sample be brought up close to room temperature for about two hours while insulation was provided. It is seen from Figure 7 and the curve in Figure 8 that this produced an error of about 5 per cent in the magnitude of f(n). The general shape of

---

[5]Brown, Fletcher, and Wright, loc. cit.

the curve however, is not altered. The error is equivalent to that produced by a twenty minute anneal at 330°K. This is a negligible error in $\tau_{\frac{1}{2}}$ at 401°K.[6]

Samples J and O were irradiated separately and were annealed in different oil baths. The curves reproduce exactly for short times. The saturation plateaux differ, but the values for $\tau_{\frac{1}{2}}$ are essentially the same. This is an indication of the reproducibility of $\tau_{\frac{1}{2}}$.

A plot of log $\tau_{\frac{1}{2}}$ vs $10^3/T$ is shown in Figure 9. The lower temperature region shows a slope of approximately 1.2 ev. The higher temperature region has a slope of about 0.8 ev. The data points fall along a curve of the type which would be produced by two competing reactions with different activation energies.[7] A line with a 1.0 ev slope is drawn through the intersection for comparison purposes.

These data are in qualitative agreement with the results of Ishino, Nakazawa, and Hasiguti.[8]

Ishino, et al., conducted their irradiations at 293°K. In addition, these samples were allowed to stand several days before annealing. Consequently the low temperature processes had time to reach some sort of equilibrium before the annealing began. Hence the details of the data might be expected to differ from the results obtained in the work dis-

---

[6] W. L. Brown and R. C. Fletcher, Phys. Rev. 92, 591 (1953).

[7] Arthur A. Frost and Ralph G. Pearson, Kinetics and Mechanisms, (John Wiley and Sons, Inc., New York, 1958), pp. 24, 25.

[8] S. Ishino, F. Nakazawa, and R. R. Hasiguti, "Annealing of Gamma Ray Irradiated n-type Germanium." To be published.

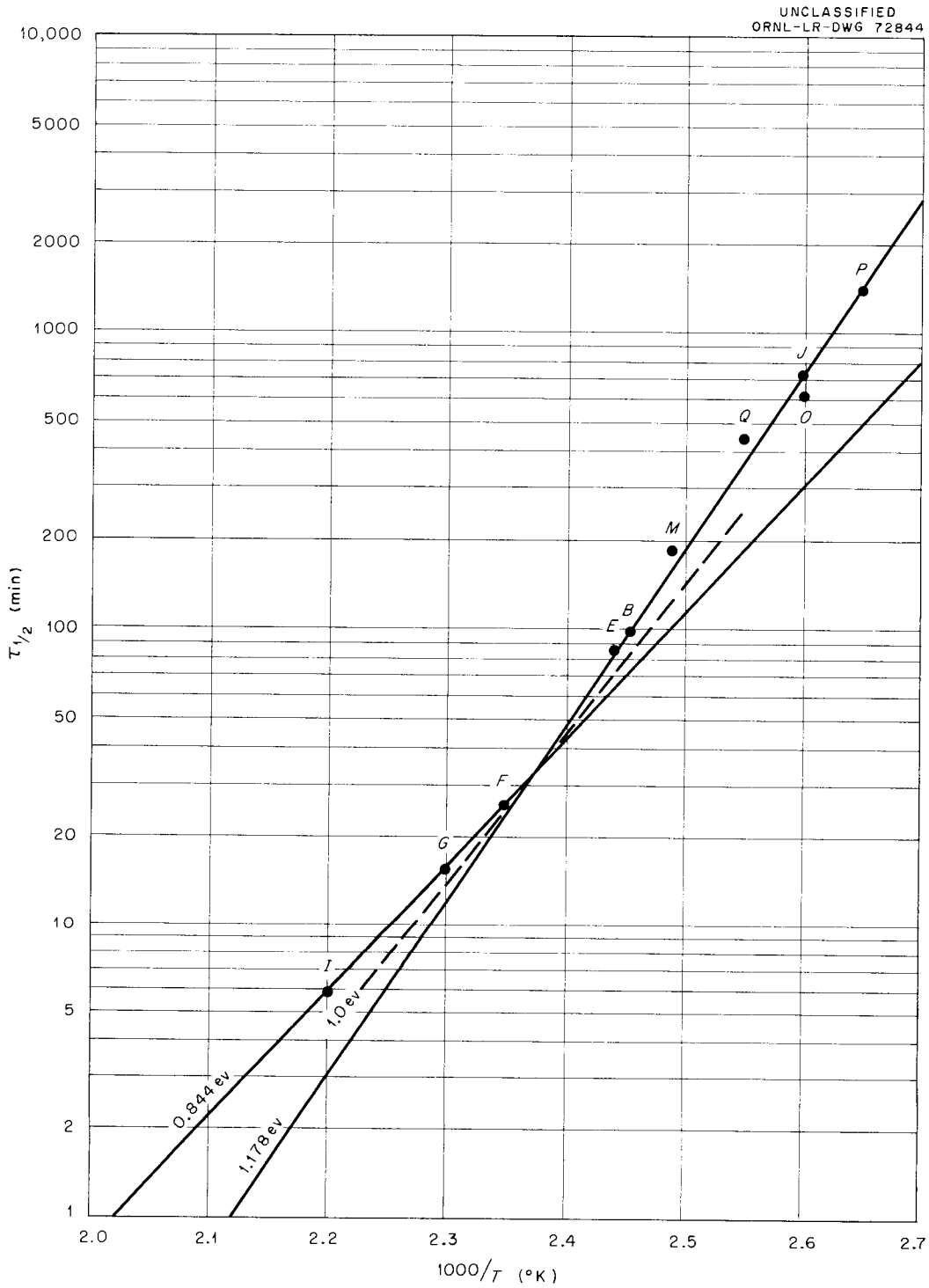

Figure 9. Log $\tau_{\frac{1}{2}}$ vs $\frac{10^3}{T}$ for the 77°K measurement.

cussed here. They did, however, find a multi-step annealing behavior and calculated a spread of activation energies ranging from 0.81 ev to 1.43 ev. They obtained these values by plotting the log of the time required for f(n) to reach a pre-determined value against the reciprocal of the annealing temperature. The value of 0.81 ev was obtained for f(n) = 0.7. The value of 1.43 ev was obtained for f(n) = 0.05. Intermediate values of f(n) gave intermediate values for the activation energy.

The activation energies were calculated for arsenic doped samples. However, the energy of motion of a vacancy through the lattice should be independent of the type of impurity. The activation energy for annealing should involve the energy of motion as well as the binding energies of any complexes formed. The lowest value of 0.8 ev obtained by Ishino, et al., agrees with the data reported here as well as that of Brown, et al., and Curtis.

A plot of the log of the saturation plateau as a function of $10^3/T$ is shown in Figure 10. The plateau value of sample M is known to be in error. Sample B was annealed in the heater in the magnet before the oil baths were constructed. Consequently the heating rate was slower for this sample than those plunged in oil. From the observations in the attempts at annealing the plateaux in samples P and O it can be inferred that the annealing produced at lower temperature during the heating process results in the production of some sort of complex which does not anneal at higher temperatures. Consequently a higher value for a plateau would have been expected in a sample annealed in the manner of sample B

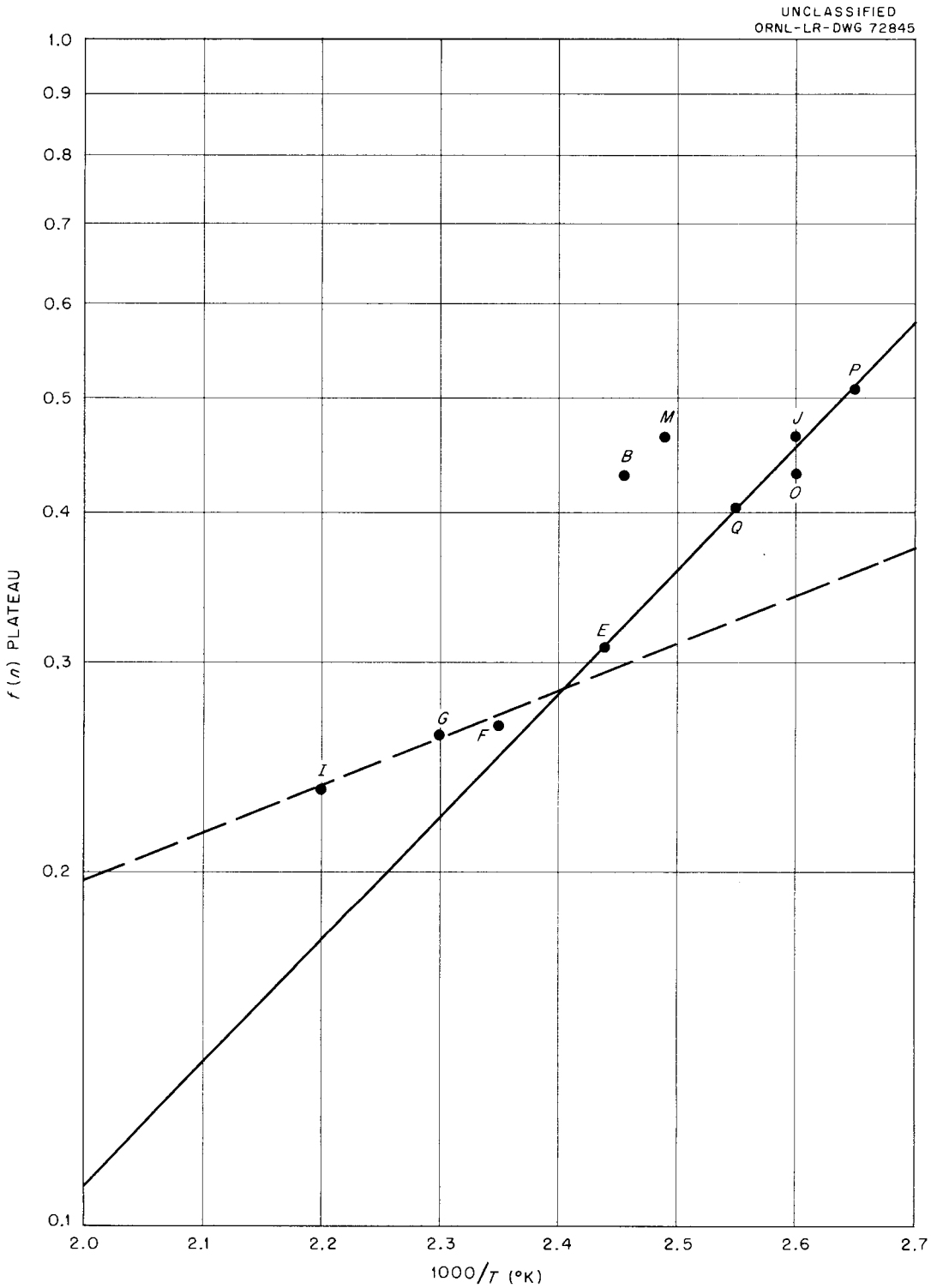

Figure 10. Saturation plateaux at 77°K.

than for a sample annealed using a faster heating rate. The resolution of the data into two distinct slopes is more pronounced in Figure 10 than in Figure 9.

The complete isochronal annealing curves for samples P, J, O, Q, M, B, E, F, G, and I are given in Figures 11 through 20, respectively. The values of f(n) are given for the $77^{o}K$ value which includes both the deep and shallow levels, the $273^{o}K$ reading which measures only the deep level, and the shallow level which is obtained from the difference in carrier concentration observed between the $273^{o}K$ and $77^{o}K$ readings.

The saturation plateau for the $273^{o}K$ reading or deep level was always higher than that for the $77^{o}K$ reading. The shallow level usually reached a saturation plateau around f(n) of 0.2 with the exception of samples B and E. As the annealing temperature was increased, the difference between the saturation plateaux decreased. This would indicate that the deep level was more stable than the shallow level.

The values of the log of $\tau_{\frac{1}{2}}$ for all three conditions are plotted against $10^3/T$ in Figure 21. There seems to be little difference in the behavior of $\tau_{\frac{1}{2}}$ for either level.

C. Mobility Changes

The values of $f(\frac{1}{\mu})$ for the isochronal anneal of EP8-K are shown in Figure 22. The changes in mobility were small. Consequently the scatter in the data was amplified when $f(\frac{1}{\mu})$ was computed. Comparison with other data, however, suggested that the results were valid within the limits of the solid lines and that the general shape of the curve is correct. Approximately 25 per cent of the induced mobility change

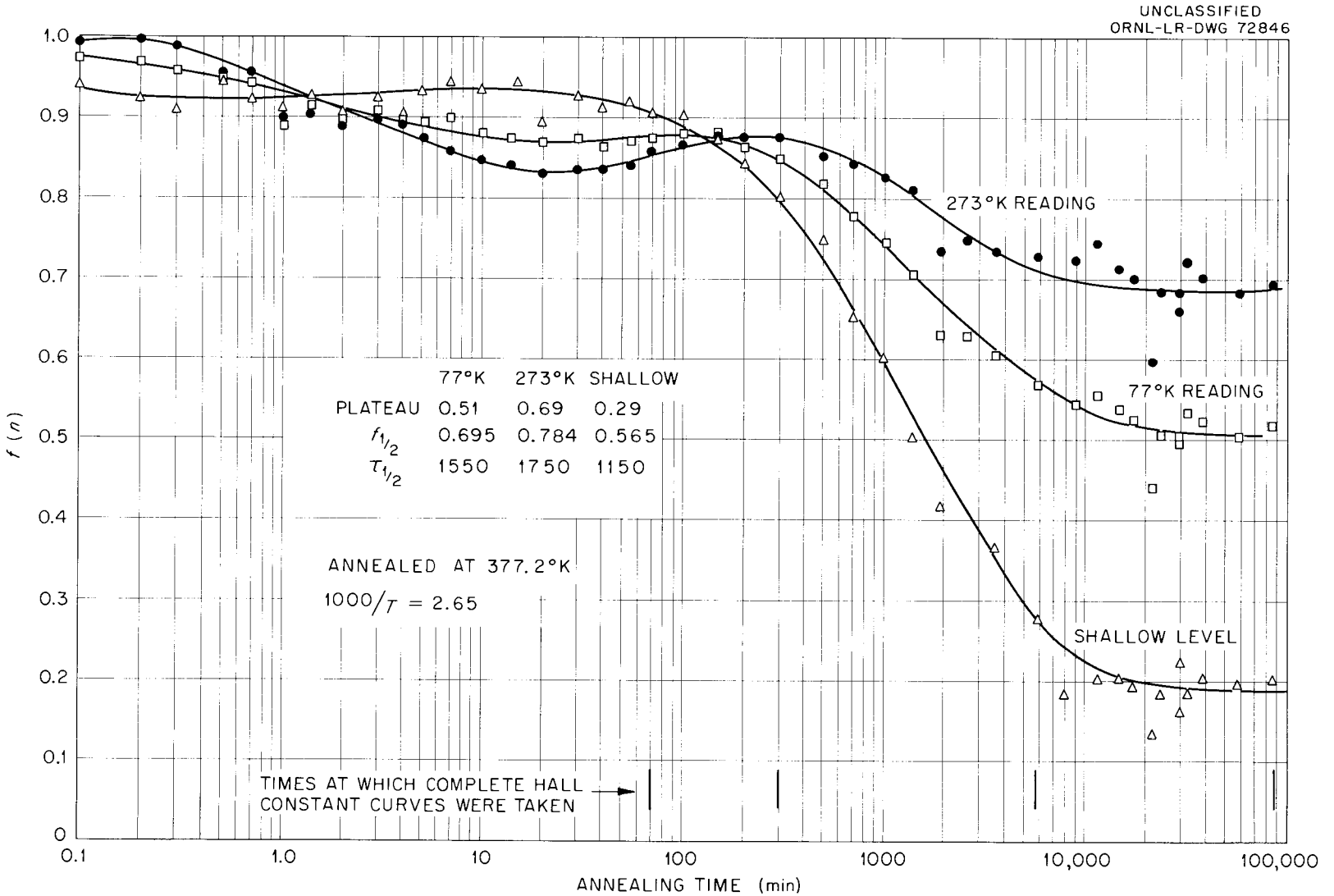

Figure 11. Isothermal anneal at 377.2°K EP8-P.

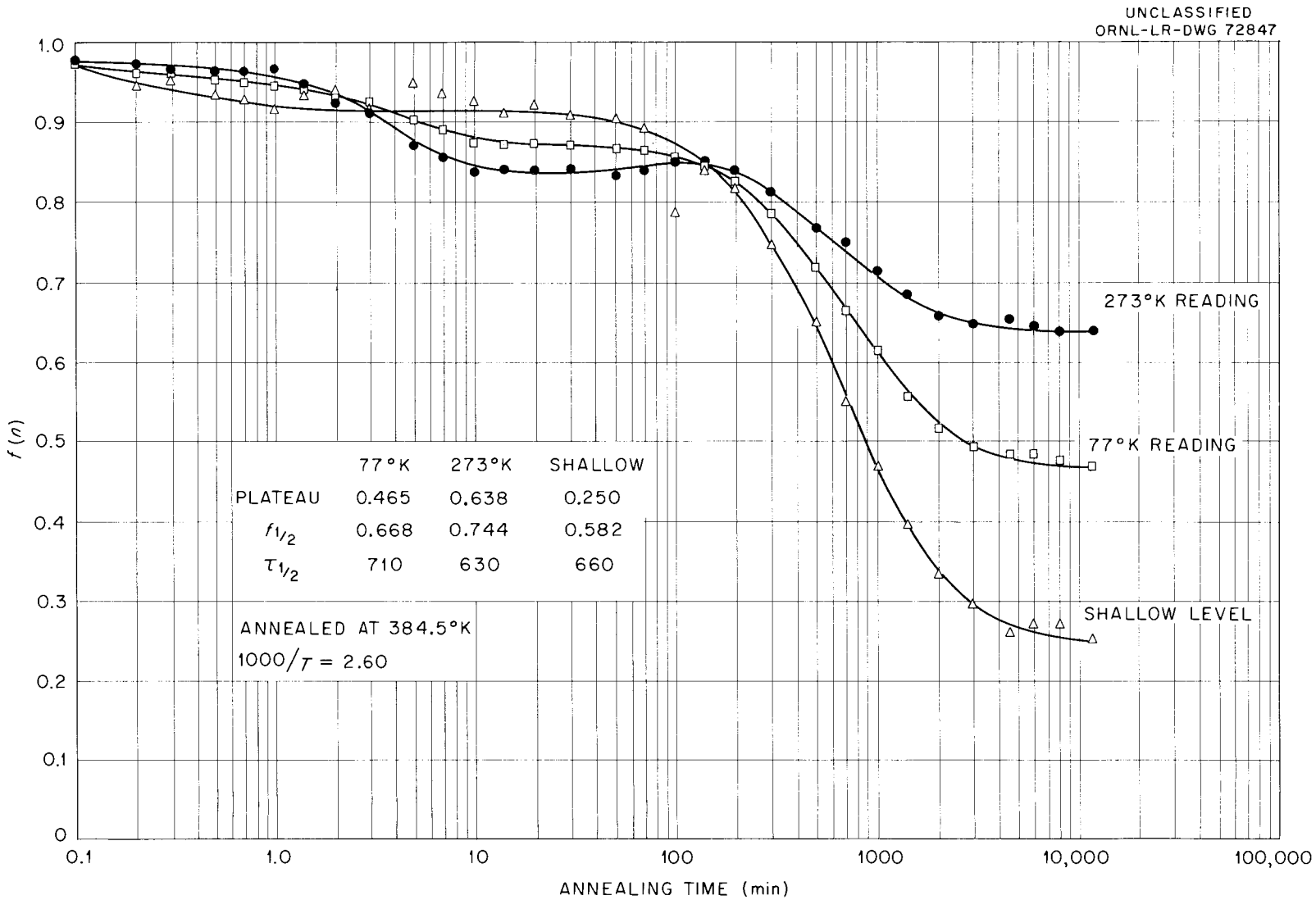

Figure 12. Isothermal anneal EP8-J.

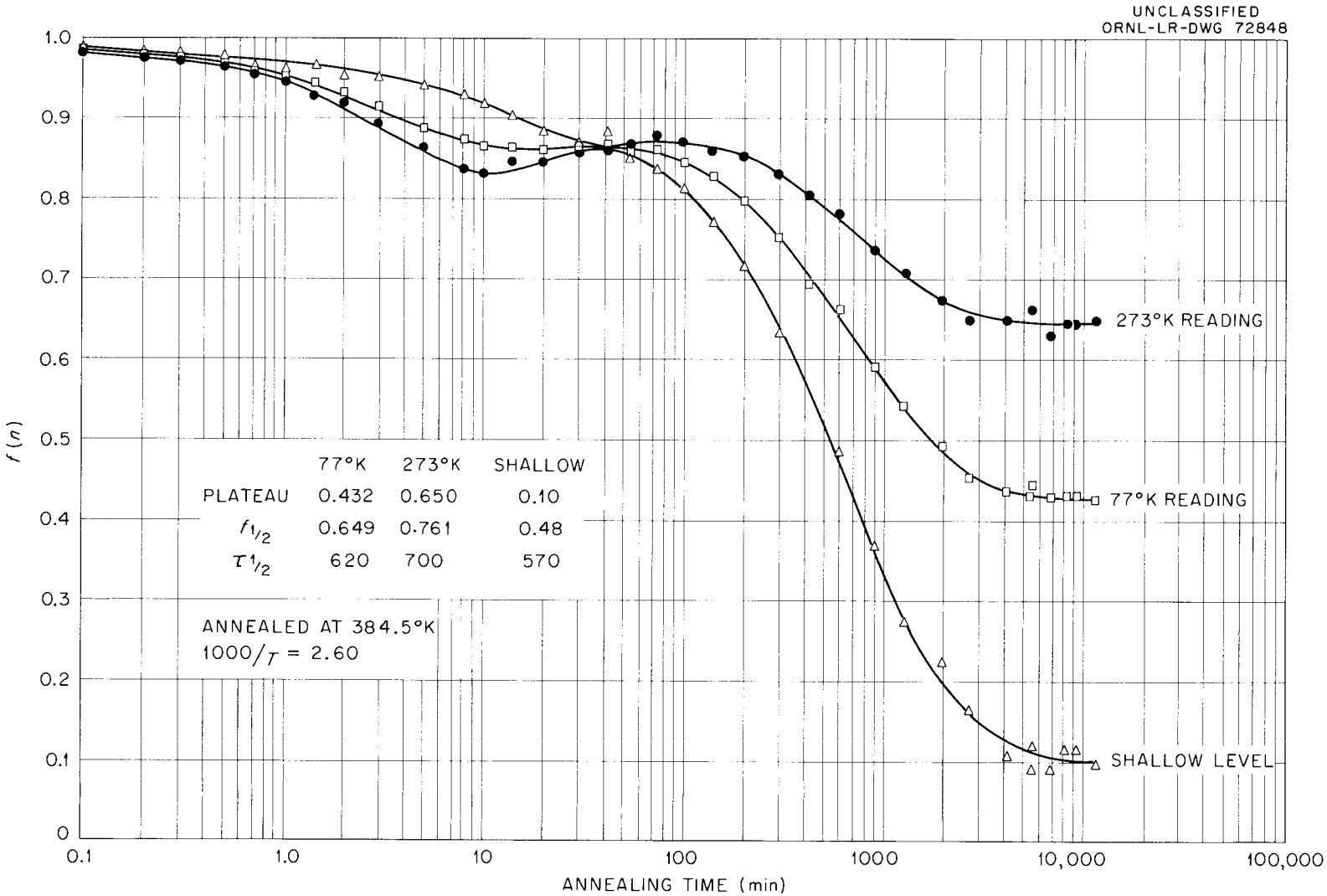

Figure 13. Isothermal anneal EP8-0.

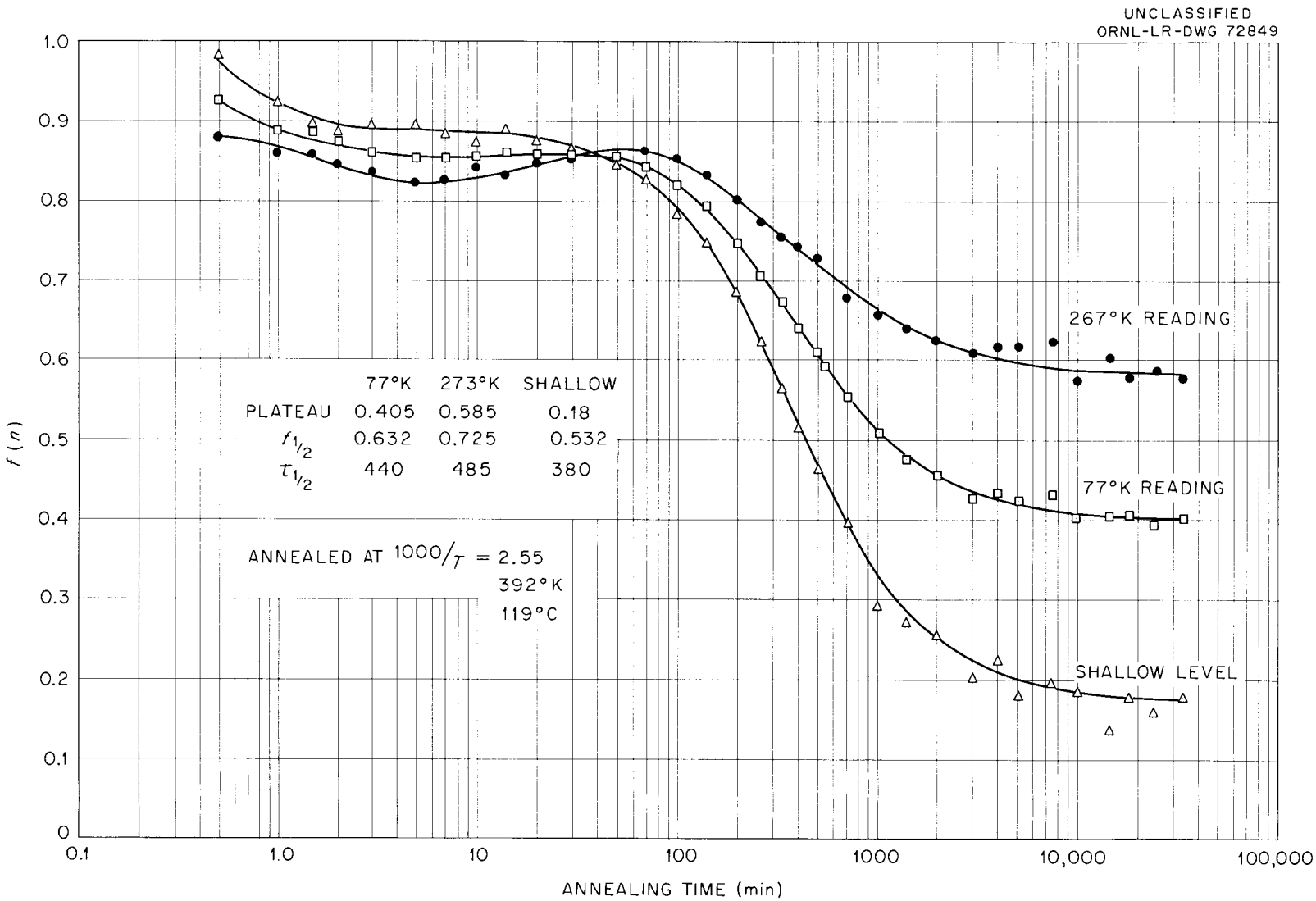

Figure 14. Isothermal anneal EP8-Q.

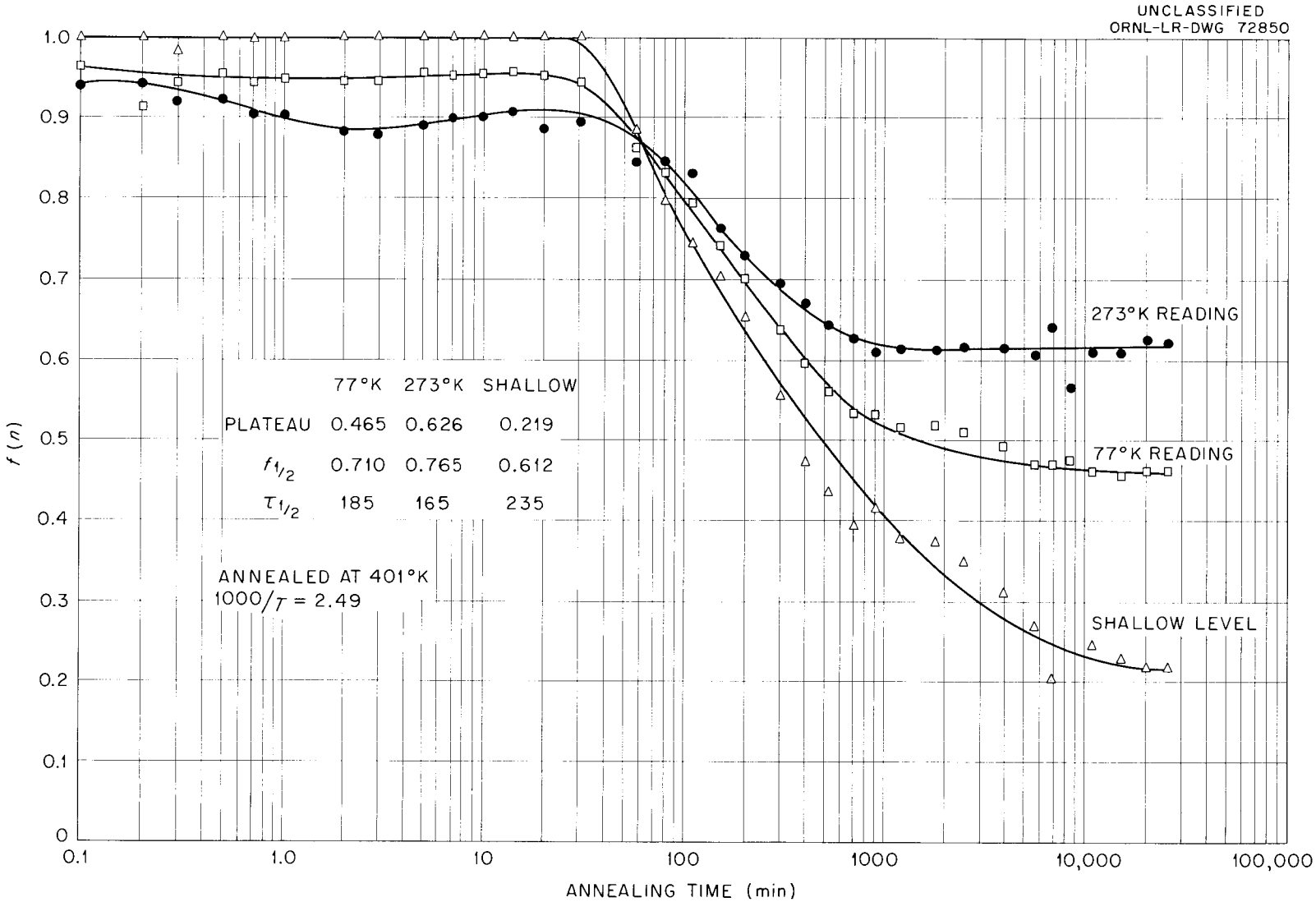

Figure 15. Isothermal anneal EP8-M.

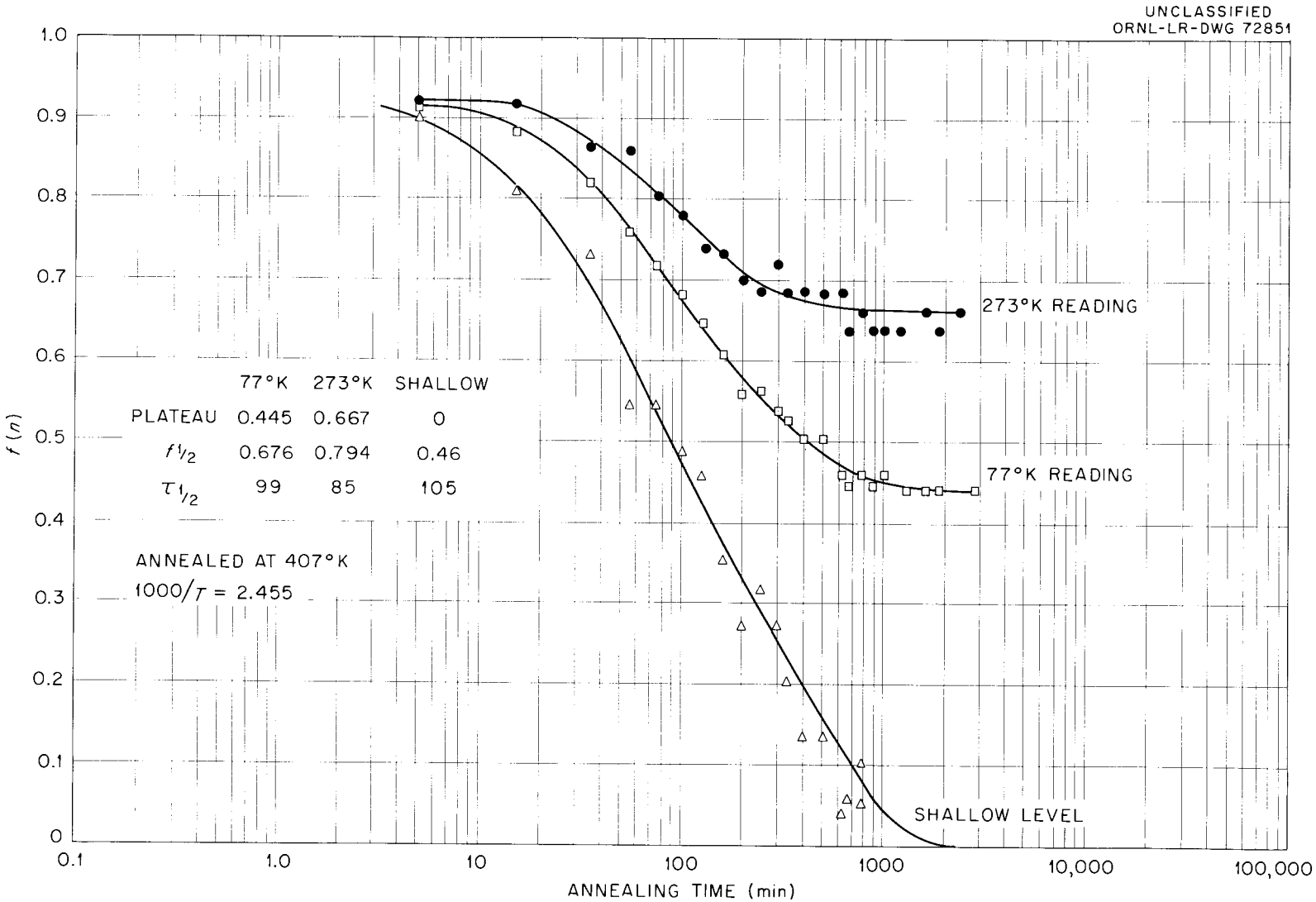

Figure 16. Isothermal anneal EP8-B.

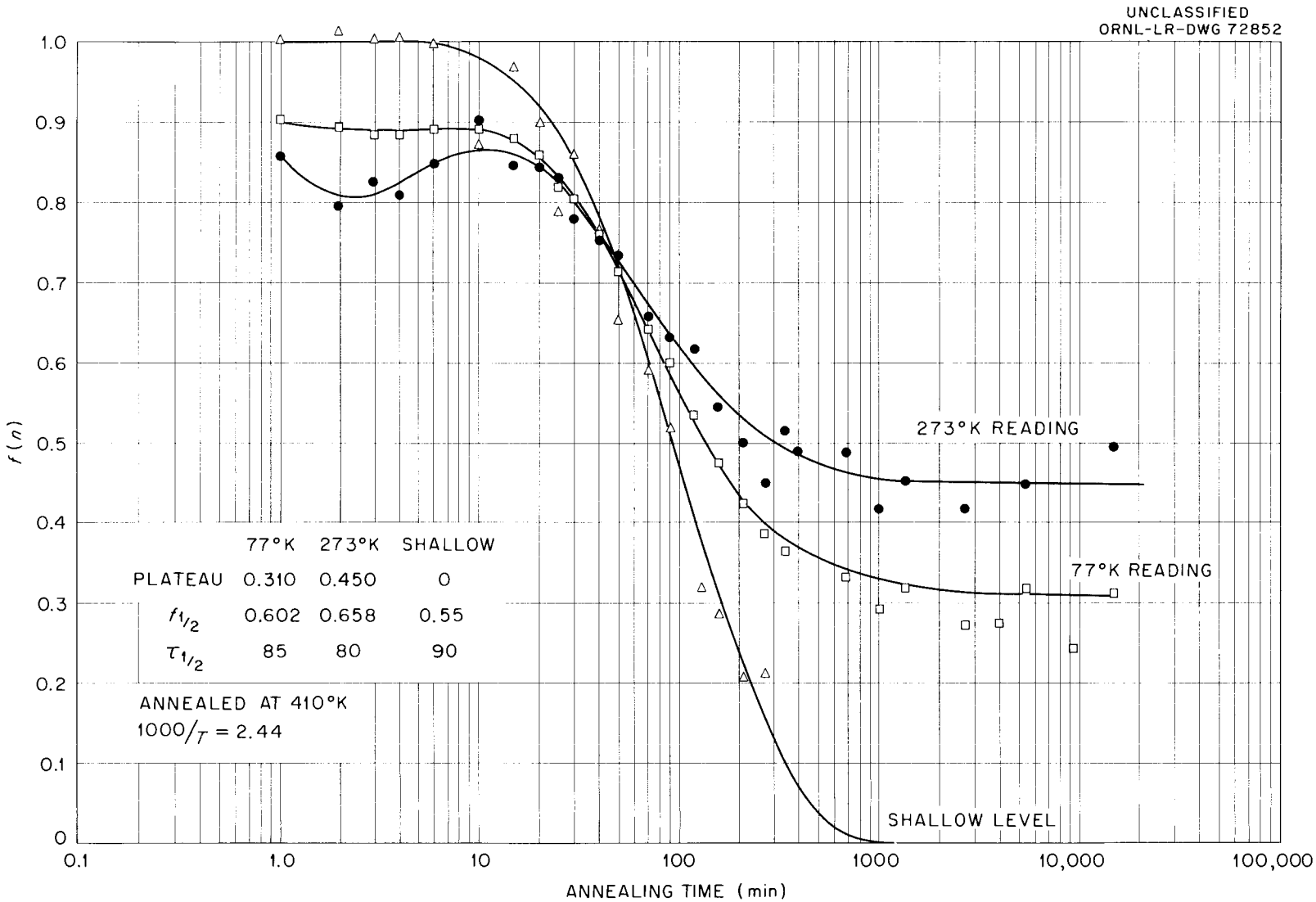

Figure 17. Isothermal anneal EP8-E.

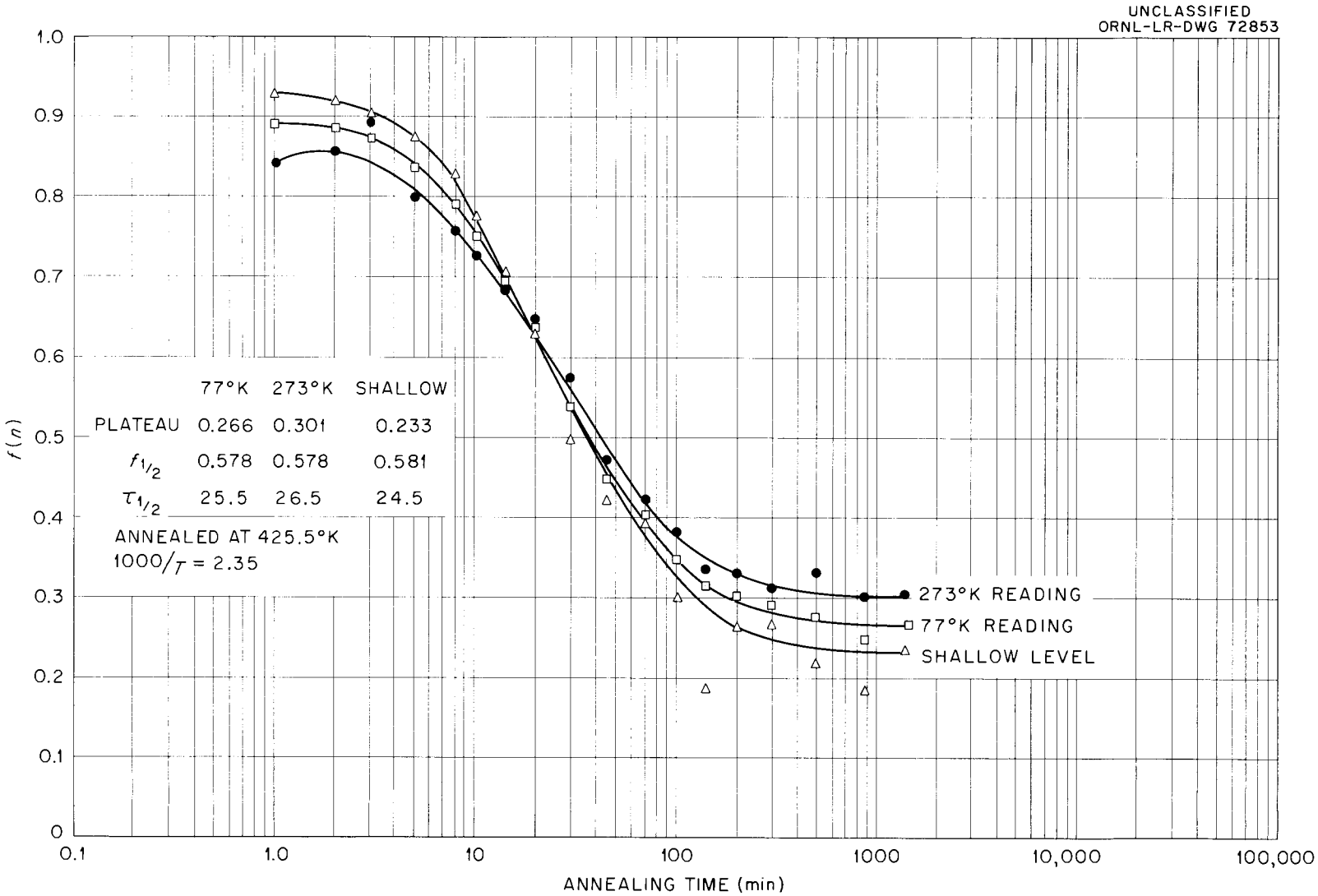

Figure 18. Isothermal anneal EP8-F.

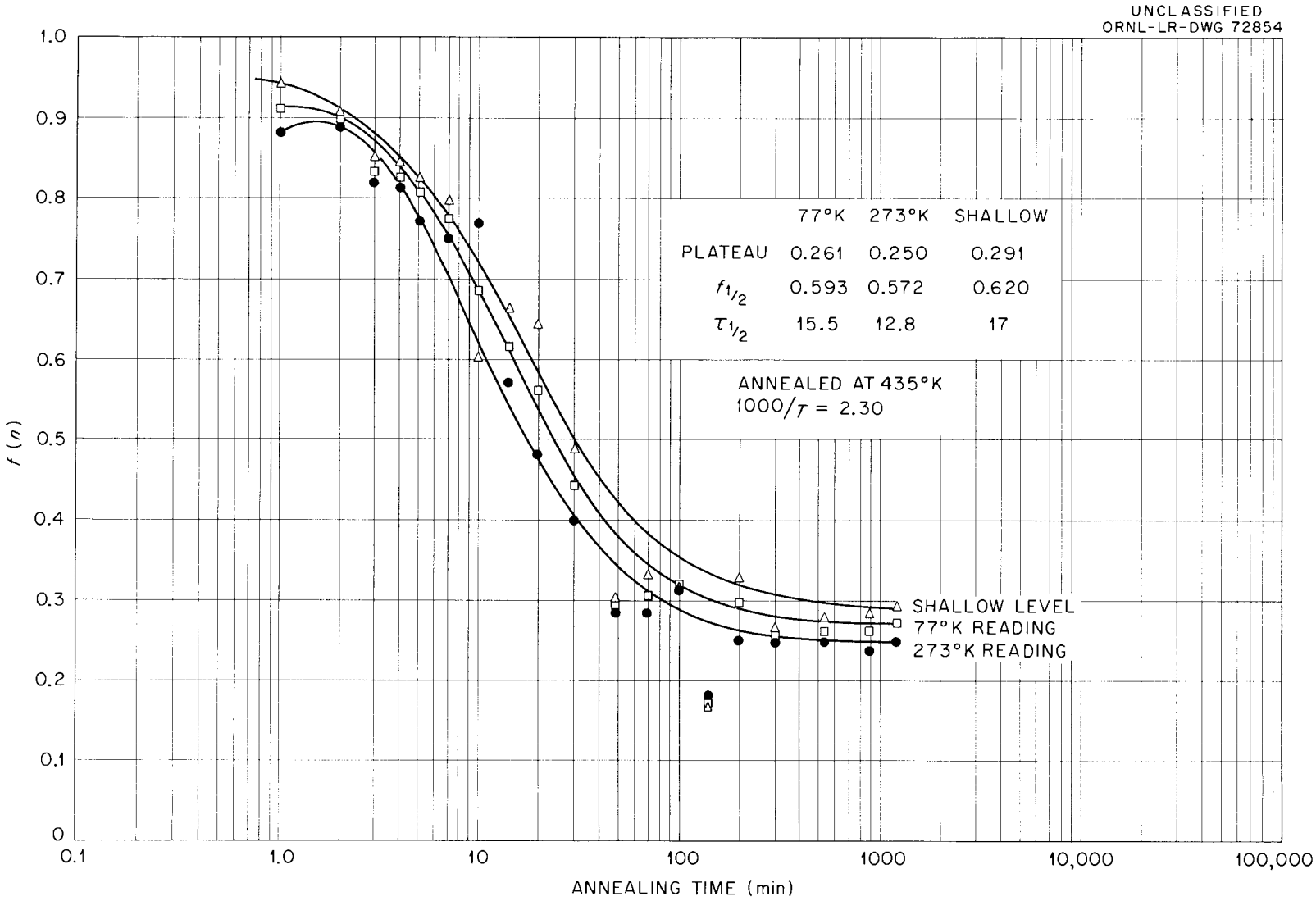

Figure 19. Isothermal anneal EP8-G.

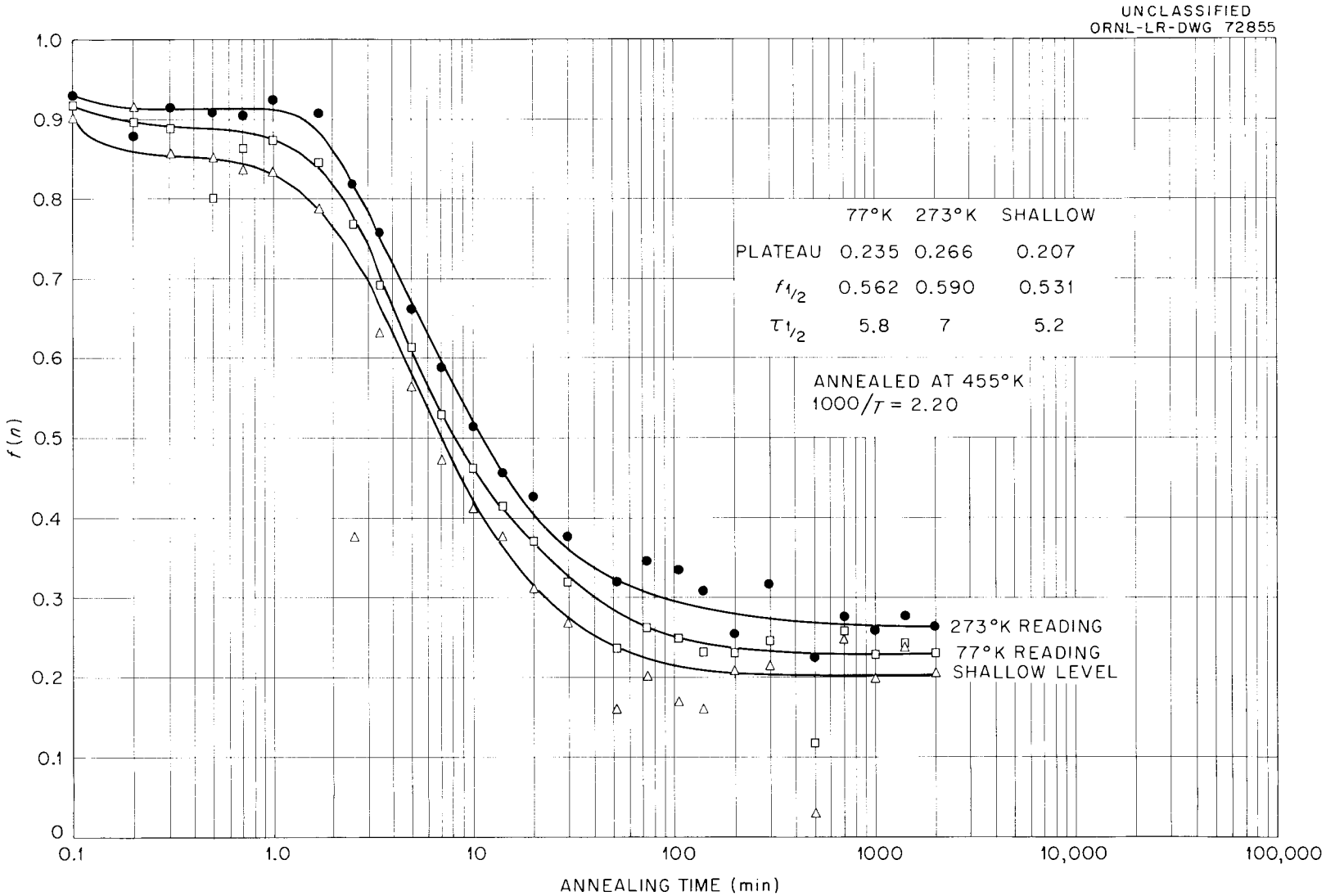

Figure 20. Isothermal anneal EP8-I.

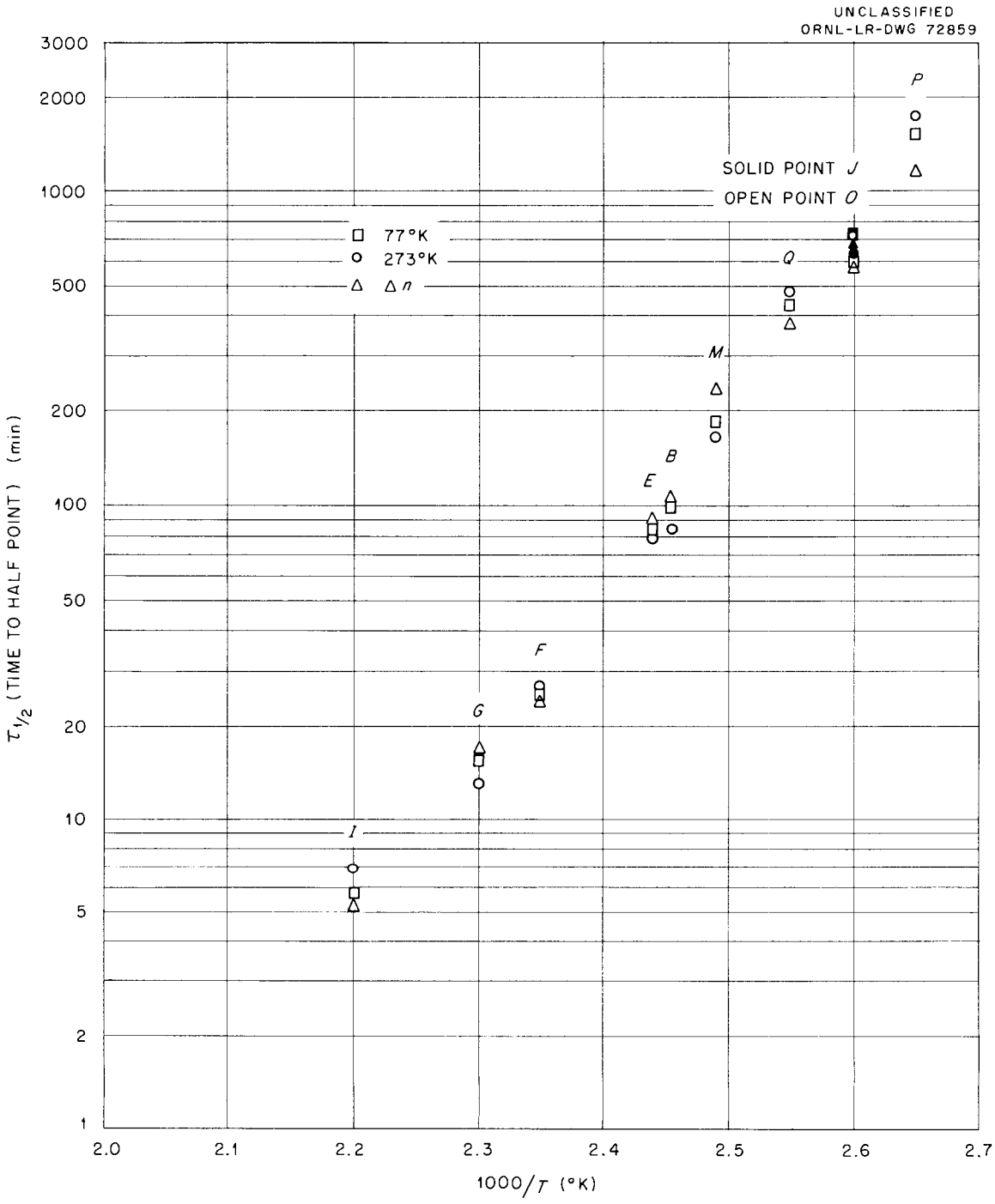

Figure 21. Composite $\tau_{\frac{1}{2}}$.

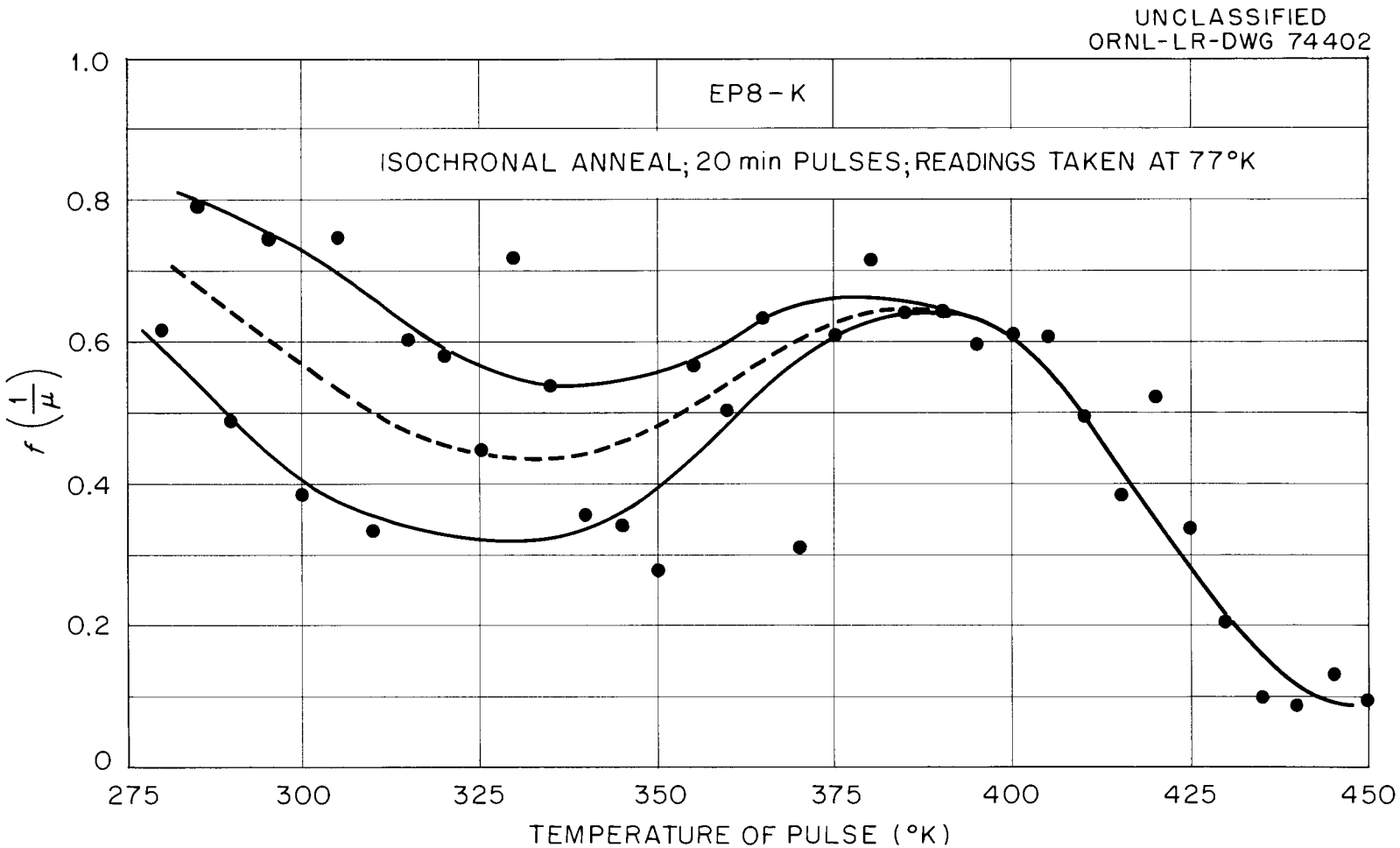

Figure 22. Isochronal anneal EP8-K.

was removed by heating to 273°K. There was a definite minimum around 340°K and a sharp break at 390°K. Approximately 90 per cent of the induced change was removed by the anneal to 450°K.

A plot of log $\frac{1}{\mu}$ vs log T for EP8-P is given in Figure 23. The data were taken before irradiation, after irradiation, and after a 70 minute anneal at 377.2°K. The change in $\frac{1}{\mu}$ over most of the temperature range has been removed except in the low temperature portion.

A plot of $f(\frac{1}{\mu})$ vs log of annealing time for sample EP8-P annealed at 377.2°K and sample EP8-F annealed at 425.5°K is given in Figure 24. The 377.2°K anneal showed two distinct steps. The final value of $f(\frac{1}{\mu})$ was approximately 0.1. The 425.5°K anneal gave a monotonic decrease in $f(\frac{1}{\mu})$ with a final value of approximately 0.025.

Since Ishino, et al., did not report mobility data, there is no opportunity for comparison.[10] However, the data shown in Figure 22 would suggest that the annealing behavior of samples irradiated at 293°K would be similar to that shown in Figure 22. There is obviously a considerable amount of annealing of the mobility change during the warm-up from 77°K to 300°K.

D. Temperature Dependence of Observed Change in Carrier Concentration

The annealing curves all showed that the annealing behavior was different when the observations were made at 77°K from that when the observations were made at 273°K. This temperature dependence was exhibited both in the change in carrier concentration during irradiation and the change

---

[10] Ishino, Nakazawa, and Hasiguti, op cit.

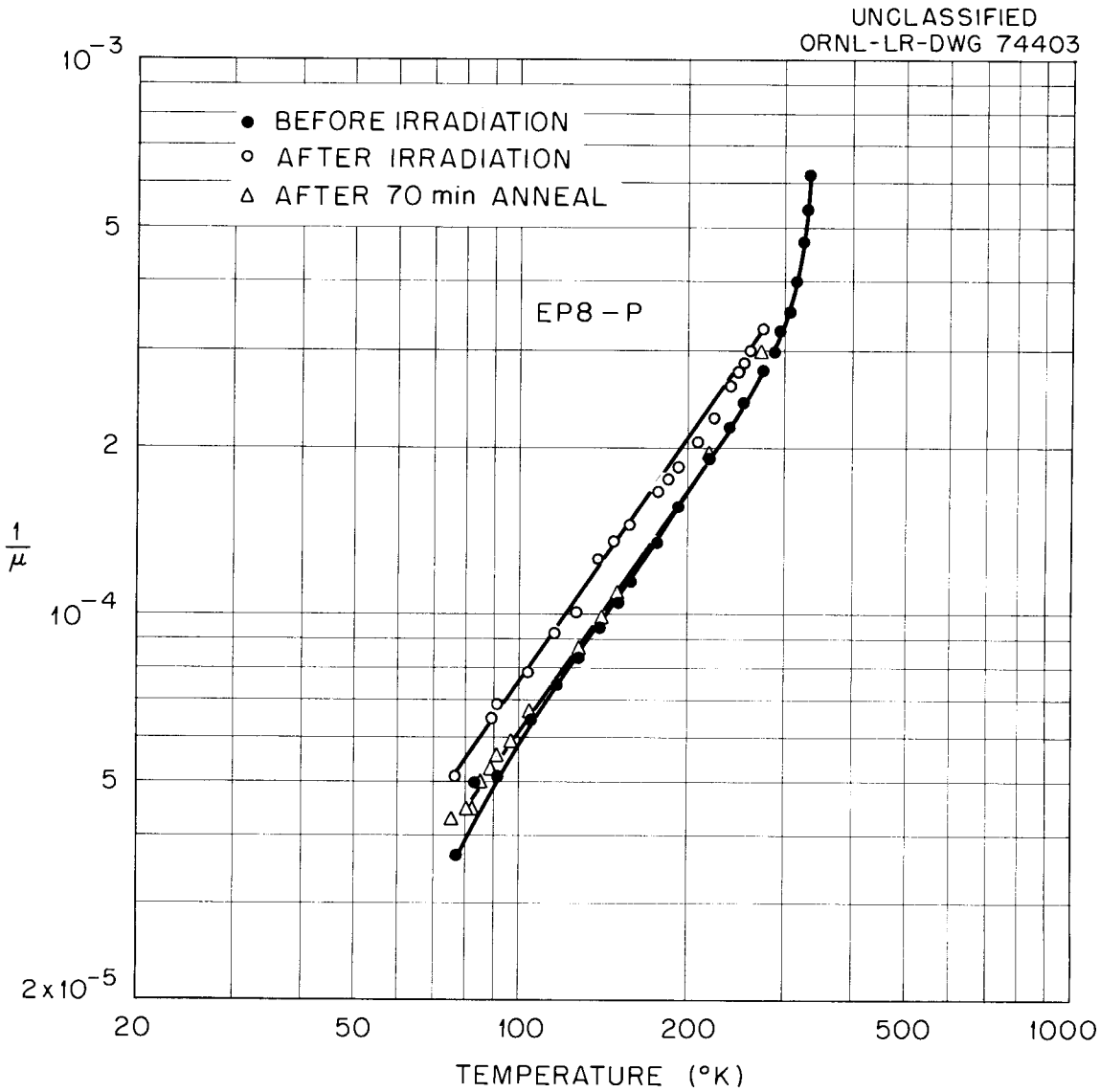

Figure 23. Log $\frac{1}{\mu}$ vs log T for EP8-P.

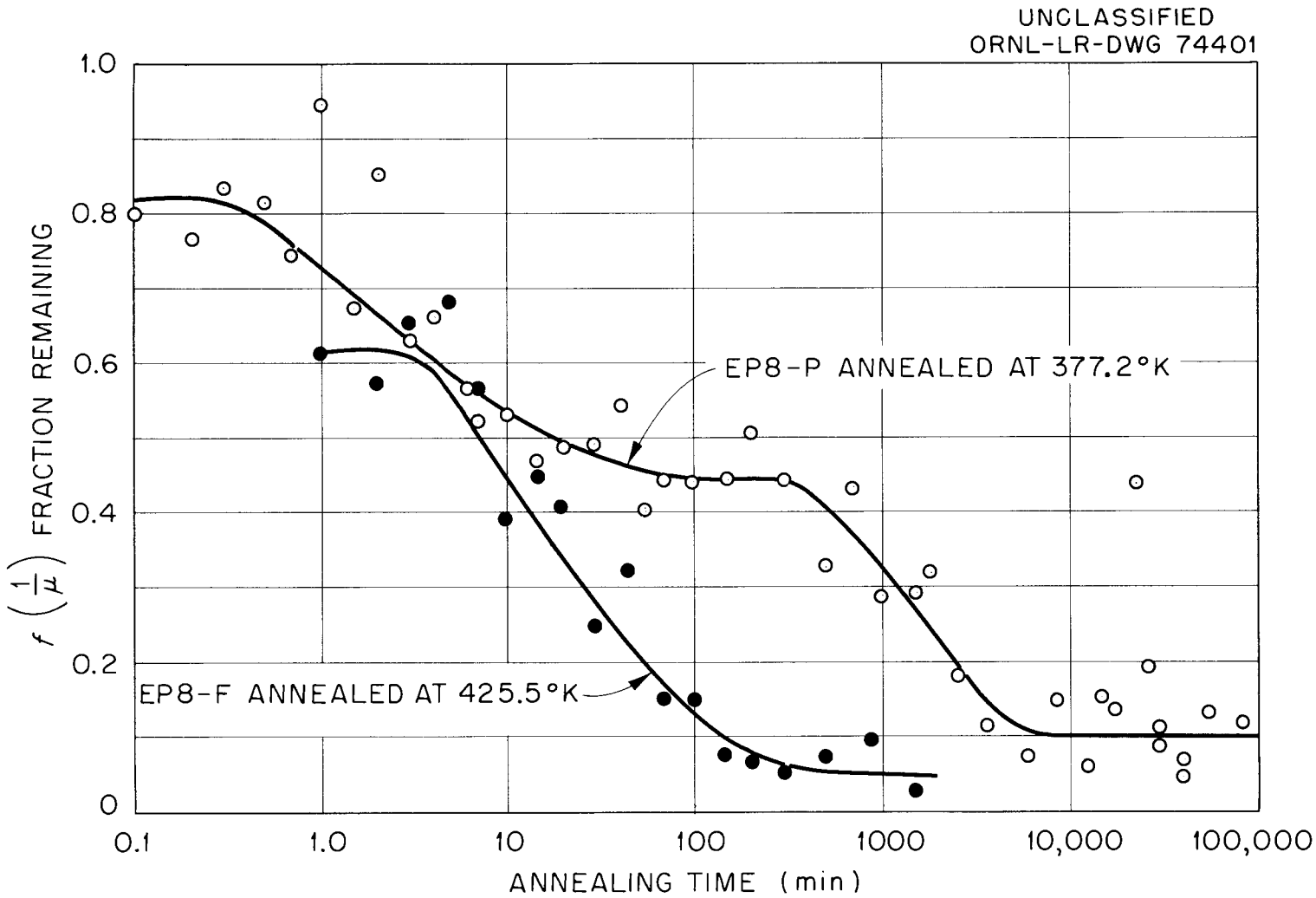

Figure 24. Isothermal anneal of reciprocal mobility.

in carrier concentration during anneal. The carrier concentration removed when measured at $77^{o}K$ and $273^{o}K$ is plotted as a function of irradiation in Figure 25. The slope of the curve measured at $77^{o}K$ is nearly twice that measured at $273^{o}K$. One can conclude that there are at least two ionization states associated with the radiation induced defects. This observation is in agreement with the data of Crawford and Cleland.[11]

Crawford and Cleland found that in germanium which had been irradiated at ambient temperature by Co^{60} gamma irradiation the change in carrier concentration changed by about a factor of two when the Fermi level crossed a level 0.2 ev below the conduction band.

The presence of the 0.2 ev level was also observed in the $77^{o}K$ irradiation. This is illustrated in Figure 26. The curves in Figure 26 were taken before and after irradiation and after an isothermal anneal. The annealing times for the sample in Figure 26 are indicated in the isothermal curve, Figure 11. The Hall curve taken immediately after irradiation showed no energy level structure between the liquid nitrogen reading and the 0.2 ev level. The Fermi level immediately after irradiation was 0.078 ev at $77^{o}K$. The curve after 70 minutes anneal at $377^{o}K$ was taken after the short time process was essentially complete. A distinct level at 0.09 ev was produced by this first stage annealing. The concentration of this level corresponded to a change in the carrier concentration of approximately 8×10^{12} electrons cm^{-3}. The strength of this level in terms of change in carrier concentration remained

---

[11] J. H. Crawford, Jr. and J. W. Cleland, J. Appl. Phys. 30, 1204 (1959).

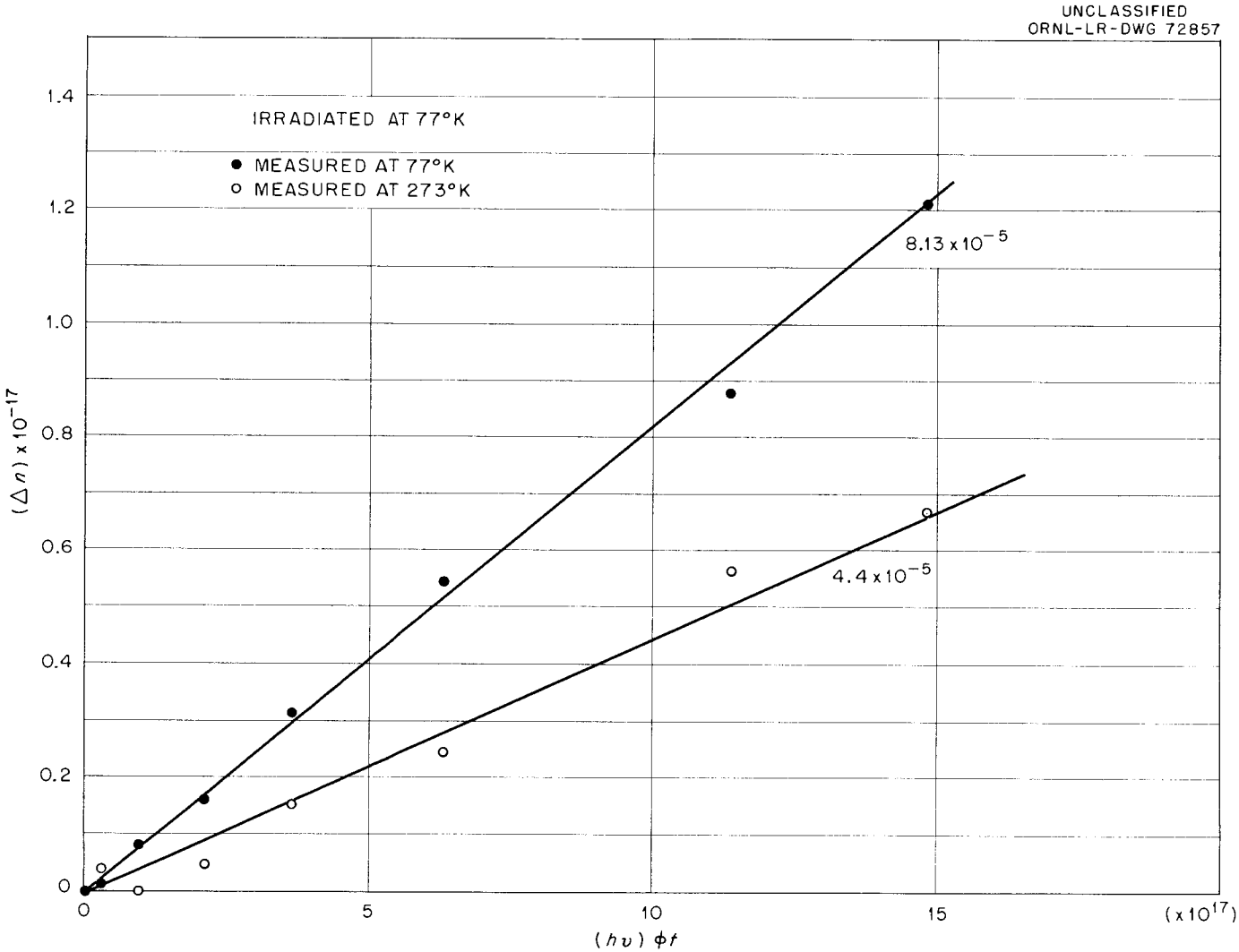

Figure 25. Carrier concentration removed vs Co^{60} gamma irradiation.

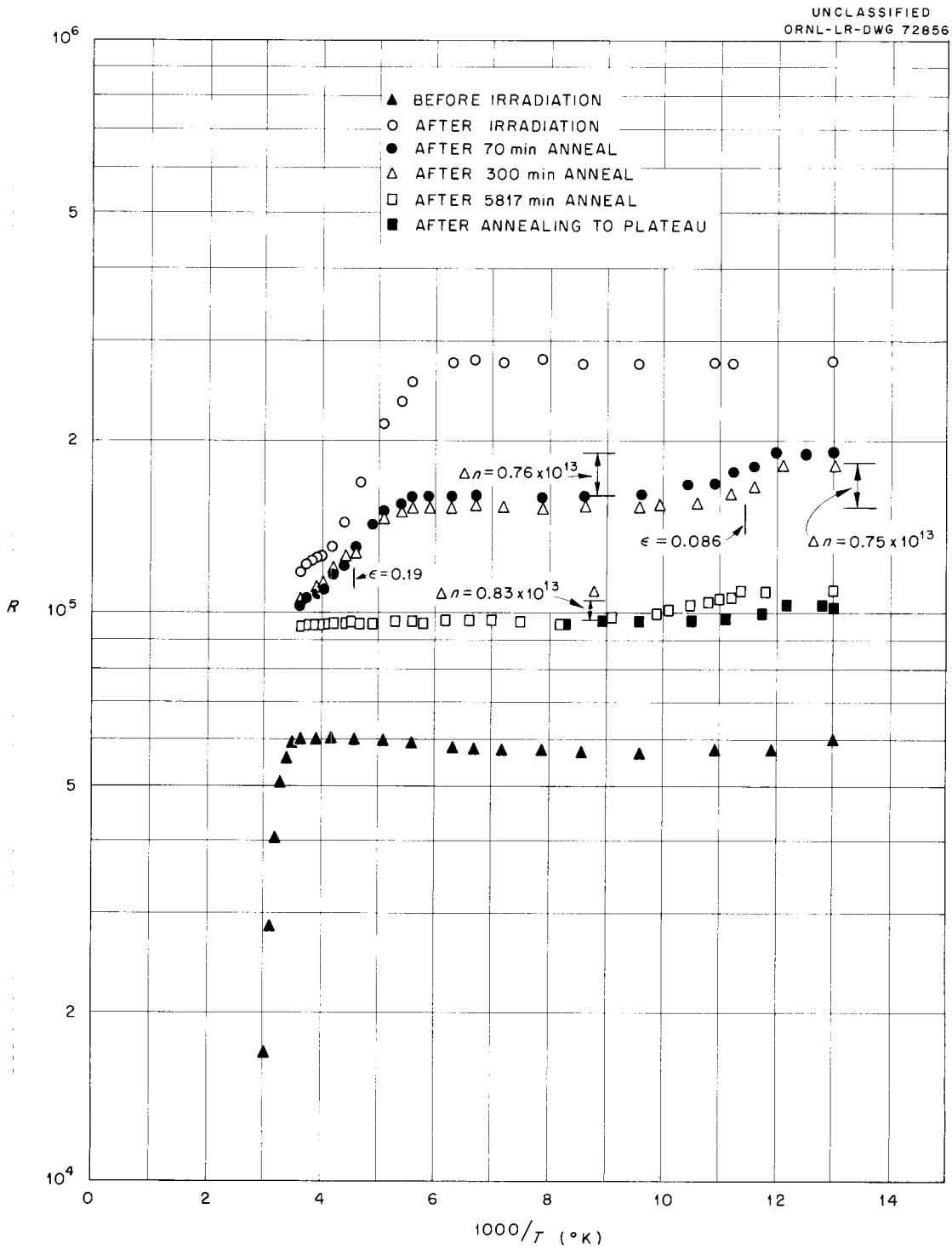

Figure 26. Effect of irradiation and anneal on the Hall constant EP8-P.

essentially unchanged throughout the major annealing process.

A level at 0.09 ev has been reported by Fan and Lark-Horovitz in electron irradiated n-type germanium.[12] The level was observed using photo-conductivity techniques with n-type germanium that had been irradiated with 4.5 Mev electron irradiation.

---

[12] H. Y. Fan and K. Lark-Horovitz, "Irradiation of Semiconductors," Semiconductors and Phosphors, M. Schön and H. Welker (editors), (Interscience Publishers, Inc., New York, 1958), p. 121.

CHAPTER IV

DISCUSSION

A. Summary of Experimental Results

1. States observed. Examination of the Hall effect curve, Figure 26, and the curve for the change in carrier concentration during irradiation, Figure 25, reveals that two acceptor states are introduced by the irradiation. One state is located approximately 0.2 ev below the conduction band. The other state is located near or below the middle of the forbidden band. The 0.2 ev level may be referred to as the shallow state and its concentration designated N_s. The deep level may be referred to as the deep state and its concentration designated N_d. One may conclude from Figure 25 and Figure 26 that the Co^{60} gamma irradiation at $77^{o}K$ resulted in the introduction of these states in approximately equal concentrations. A new state at 0.09 ev below the conduction band appeared after a short anneal. This state was not observed in measurements made after irradiation but before anneal.

2. Isochronal anneal. Examination of the isochronal curves reveals that first a decrease in the concentration of deep states was observed followed by an increase which persisted until approximately $390^{o}K$. In subsequent annealing at higher temperatures, the total concentration of states (N_T) and the concentration of deep states annealed together.

During the anneal up to $320^{o}K$, there was a definite decrease in

the concentration of the deep states. However, some process also occurred involving the shallow states in such a manner that the total concentration of states remained unchanged.

The concentration of total states showed a sudden decline at 320°K which changed the concentration by about 4 per cent. There was no further change in total state concentration until 380°K. The concentration of deep states went through a minimum at approximately 370°K and then rose sharply to a maximum at 395°K. Since the total state concentration did not change in this interval, this suggests that the deep state concentration was increased at the expense of the shallow state concentration. Formation of complexes by the more mobile constituent with a consequent depression of the 0.2 ev state is a possible process to account for the increase. The minor 4 per cent decrease in the total state concentration suggests annihilation of the mobile constituent either at a sink or by its opposite member in the manner proposed by Reiss.[1] The qualitative behavior of the effective concentration change of the scattering centers as measured by the reciprocal mobility was similar to that observed for the deep states. This change in reciprocal mobility is shown in Figure 22. There was a minimum in $f(\frac{1}{\mu})$ in the same temperature range as the minimum in $f(n)_{273}$. There was also a definite break in the annealing curve at about 395°K which resulted in a monotonic decrease in the induced change for annealing at higher temperatures.

---

[1]H. Reiss, J. Appl. Phys. 30, 1141 (1959).

The decrease in $f(\frac{1}{\mu})$ is essentially twice the decrease in $f(n)_{273}$. The value of $f(n)_{273}$ for the minimum at 370°K had decreased by about 20 per cent. The value of $f(\frac{1}{\mu})$ at the same point had decreased over 50 per cent. The resultant decrease in $f(n)_{273}$ for the maximum at 395°K was about 11 per cent. The value of $f(\frac{1}{\mu})$ maximum at 395°K represented a resultant decrease of about 35 per cent. These values of $\frac{1}{\mu}$ were measured at 77°K. The total carrier concentration as represented by f(n) measured at 77°K was essentially constant in this temperature range. These observations suggest that the process involved in changing the concentration of the deep state also produced the large change in the effective scattering center concentration. Since the magnitude of the percentage change in scattering is approximately twice that of the percentage change in the deep state concentration, some process which pairs up negative and positive charges suggests itself.

Since prior work does not indicate that interstitials form complexes with substitutional antimony atoms, it is difficult to specify the nature of the complex. The formation of oxygen-interstitial or vacancy-interstitial complexes could give a possible explanation to the observed behavior. A di-interstitial or a cluster of interstitials could be expected to have different scattering properties from those of isolated interstitials. The scattering seems to be of the Conwell-Weisskopf type, however, and the absence of any direct evidence for the presence of ionized interstitials tends to rule against this assumption. The formation of vacancy-antimony complex would produce the observed mobility change by converting scattering centers from isolated charges to a dipole plus a singly charged monopole. The induced mobility change would thus be reduced without

changing the carrier concentration.

The increase in the deep state concentration in the region between 360°K and 390°K without a corresponding change in the total state concentration indicates that deep states are being produced at the expense of shallow states. The conversion of shallow states to deep states has been observed by Cleland, Crawford, and Holmes, and by Crawford and Cleland in gamma irradiated n-type germanium with unspecified impurity content.[2,3] Further confirmation of this form of isochronal annealing has been obtained by Oka by following the Hall coefficient at the triple point of water.[4]

Isochronal anneal in the temperature ranges above 390°K resulted in the recovery of the total state concentration along with the deep state concentration. The recovery is 60 per cent complete after annealing at 450°K. This agrees with the data of Ishino, et al., on antimony-doped germanium for the anneal of the total state concentrations.[5]

3. Isothermal annealing. It is clear from Figure 9 that the annealing behavior was of two types, one type predominated for low anneal-

---

[2] J. W. Cleland, J. H. Crawford, Jr., and D. K. Holmes, Phys. Rev. 102, 722 (1956).

[3] J. H. Crawford, Jr. and J. W. Cleland, J. Appl. Phys. 30, 1204 (1959).

[4] M. Oka, Shimane University, Japan, (unpublished data).

[5] S. Ishino, F. Nakazawa, and R. R. Hasiguti, "Annealing of Gamma Ray Irradiated n-Type Germanium," (to be published).

ing temperatures in the range of 400°K and below. The other predominated for high temperatures at 425°K and above. The data in Figure 8 shows that the general characteristics of the annealing curve for the total state concentration differed in these two temperature ranges.

There was an early plateau in the low temperature anneals followed by a general anneal and ending in a saturation plateau. The saturation plateau was temperature dependent. The value of the plateau was lower for higher annealing temperatures. Once the plateau was established, however, it was stable for anneals at higher temperature. A sample annealed to the saturation plateau at 355°K would show no change upon subsequent anneal at 455°K.

The behavior shown in Figure 11 was typical in the low temperature range. The value of the saturation plateau for the shallow level concentration was about 0.2. The saturation plateaux for the deep state concentration and the total state concentration were successively lower for higher temperatures, but the difference in the plateaux were consistent. The plateau for the deep level was higher than that of the total state concentration by about 18 per cent of the initial concentration.

The temperature dependence of the saturation plateaux in the higher temperature region were considerably less temperature dependent than in the low temperature range. This is illustrated in Figures 8 and 10.

The behavior shown in Figure 20 was typical for samples in the high temperature range. The value of the saturation plateaux for the shallow levels were again 0.2. The saturation plateaux for the deep

state concentrations were again higher than for the total concentration, but the difference in the value is now of the order of 5 per cent of the initial concentration. With the exception of this consistent difference, the curves for the shallow state, deep state, and total state concentrations were consistently of the order of 7 per cent in the high temperature range. Figure 26 shows that the value of 7 per cent for the difference can be explained by the presence of the 0.09 ev level which is stable during the anneal.

A two stage process was observed in the annealing of the reciprocal mobility in the low temperature range. The plateau shown in Figure 24 occurred at a value of $f(\frac{1}{\mu})$ of about 0.5. The final plateau of $f(\frac{1}{\mu})$ was about 0.1. Comparison of Figure 24 and Figure 8 indicates that half the change in $(\frac{1}{\mu})$ was removed by the anneal that removed only about 12 per cent of the total induced state concentration. At the final plateau, 90 per cent of the induced change in $\frac{1}{\mu}$ had been removed but only 50 per cent of the change in total state concentration was removed.

The corresponding plateaux in the high temperature range were 0.05 for $f(\frac{1}{\mu})$ and 0.25 for $f(n)$. There was a 95 per cent removal of the induced mobility change and a 75 per cent removal of the total state concentration.

The activation energies for the anneal as shown in Figure 9 were 0.844 ev in the high temperature range and 1.178 ev in the low temperature range. The compilation of data in Figure 21 shows that the activation energies would have been the same had they been computed from the

deep state concentration or shallow state concentration instead of total state concentration. The data in Figures 9 and 22 represented observations of the second stage or principal anneal. Such a superposition could clearly not have occurred in the region where the removal of shallow states increased the concentration of deep states.

4. Radiation induced states. The irradiation introduced two observable states. This is shown in the plot of change of total state concentration in Figure 25. The shallow state is shown in Figure 26 to have been introduced at about 0.2 ev below the conduction band. Any other levels which may have been introduced were in such a position as to be inactive in producing changes in the carrier concentration.

B. Interpretation of the Data

1. The two induced states. Any interpretation of the annealing data must depend upon the identity of the observed states which were introduced by the irradiation. James and Lark-Horovitz developed a model in 1951 to explain the irradiation induced changes observed in germanium.[6] This model considers a uniform distribution of isolated interstitials and vacancies. The interstitial can be ionized to contribute two electrons, the vacancy can be ionized to accept two electrons. The first interstitial ionization level was located 0.2 ev below the conduction band, the second interstitial level was located 0.18 ev above

---

[6] H. James and K. Lark-Horovitz, Z. Physik. Chem. 198, 107 (1951).

the valence band. The levels associated with the vacancy were located 0.07 ev and about 0.01 ev above the valence band. The James-Lark-Horovitz model readily explains the irradiation results such as shown in Figures 25 and 26. For each interstitial-vacancy pair produced by the irradiation, two electron acceptor states and two electron donor states will be produced. When the Fermi level is above the 0.2 ev level, the two vacancy acceptor states will be ionized and two electrons will be removed from the conduction band. When the temperature is increased the Fermi level moves toward the middle of the forbidden gap. When the Fermi level falls below the 0.2 ev level of the interstitial, the interstitial is ionized and contributes one electron to the conduction band. Consequently the interstitial-vacancy pair removes two electrons when the Fermi level is above the 0.2 ev level and one electron when the Fermi level falls below the 0.2 ev level.

The James-Lark-Horovitz model, however, is inconsistent with the observed changes in mobility. The coulomb scattering should increase when the Fermi level falls below the 0.2 ev level due to the introduction of additional charged scattering centers. The data shown in Figure 23 indicated that a slight decrease in the scattering occurred in the region of 200°K for measurements made just after irradiation.

In the James-Lark-Horovitz model, if only interstitials are present, they can act only as electron donors. If only vacancies are present, they can act only as electron acceptors. Another model has been proposed by Blount.[7] The levels at 0.2 ev below the conduction band

---

[7]E. I. Blount, Phys. Rev. 113, 995 (1959). J. Appl. Phys. 30 1218 (1959).

and 0.07 ev above the valence band were assigned to the interstitial. The levels at 0.18 ev and 0.01 ev above the valence band were assigned to the vacancy. The assumption is made that any level in this model can be either an electron donor or acceptor. This restriction of the James-Lark-Horovitz model does not apply in the Blount model. As a consequence of the removal of the restriction of the behavior of the introduced levels, it is possible to consider some alternate possibilities not allowed by the James-Lark-Horovitz model.

One possibility is to assume that the vacancy and interstitial each act as an electron acceptor. Such an assumption could explain the irradiation data shown in Figures 25 and 26. Since the interstitial and vacancy would be expected to have different mobilities in the crystal, one would expect to find a two stage annealing behavior.

The radiation induced change in scattering center concentration should decrease when the Fermi level crosses the 0.2 ev level due to the removal of half the radiation produced scattering centers. The predicted change is in the direction of that observed, however, the change is extremely small.

A second possibility is to assume that the vacancy is a double acceptor and that the interstitial is electrically neutral. This assumption would imply that the 0.2 ev level is associated with the vacancy. A model of this type would satisfy the irradiation data and explain the absence of any direct evidence of the interstitial. The change in mobility would again be in the observed direction. The radiation induced change in reciprocal mobility measured at 273°K would be the same

in either model. An assumption of the interpretation of the carrier concentration is required to calculate the mobility. The calculated values using either model are only a factor of two different. This is a factor of two however in a small number which is obtained by subtracting two large measured numbers. The precision of the measurement does not permit a choice of model on the basis of mobility.

2. Requirements of a model. There are several critical characteristics which must be explained by any proposed model of the annealing mechanism. First it must include an explanation of the early anneal which results in a small change in the total state concentration and deep state concentration but a major change in the induced scattering. The second important aspect is the temperature dependent plateau which once established is stable for further annealing in the temperature range studied. Such a plateau cannot be obtained from simple interstitial or vacancy annihilation either simultaneously or individually. Complexes of some sort must be formed with the impurity atom.[8,9] At least one complex which has a high thermal stability must be formed from a two step process. The complex must be formed in greater concentration at low temperature than at high temperature. The third requirement of any proposed model is that it must explain the two activation energies observed.

---

[8] O. L. Curtis, Jr. and J. H. Crawford, Jr., Phys. Rev. 126, 1342 (1962).

[9] W. L. Brown, W. M. Augustyniak, and T. R. Waite, J. Appl. Phys. 30, 1258 (1959).

C. Possible Models

1. Short time anneal. An effective capture volume can be assigned the trapping centers or annihilation centers.[10] Defects which were produced within this capture volume will be able to move only to the capture or annihilation center. The annealing behavior has in this way been separated by Reiss into two distinct processes. The first is the capture of defects within the capture volume. The second is the diffusion of defects through the crystal until they interact with a capture or annihilation center. There is an early anneal in both the isochronal and isothermal curves which has the same magnitude for all samples. Since the impurity concentration and the defect concentration is essentially the same for all samples, this early anneal can be understood in terms of the mechanism proposed by Reiss. If both annihilation and capture can occur, some defects will be removed from the sample and others will be trapped.

2. Vacancy diffusion. The observed activation energies of 0.8 ev and 1.2 ev suggest that the annealing mechanism involves vacancy motion. Using the activation energy for self diffusion of germanium determined by Letaw, Slifkin, and Portnoy[11] of 2.98 ev in combination with the measured values of the free energy of formation of a vacancy, of

---

[10] H. Reiss, op. cit.

[11] H. Letaw, Jr., W. M. Portnoy, and L. Slifkin, Phys. Rev. 102, 892 (1956).

Mayburg and Rotondi[12] (2.13 ev), and Logan[13] (2.0 ev), one obtains an activation energy for vacancy motion of approximately 1 ev. The activation energies obtained from Figure 9 are in the range of 1 ev. The comparison of the values obtained from Figure 9 with those computed from the data of vacancy diffusion suggests that the mechanism of annealing involves vacancy motion. Measurements of annealing of cobalt-60 gamma ray induced damage in the presence of a large electric field has shown that the defects introduced by the irradiation were negatively charged.[14] A negatively charged defect also suggests that the defect is a vacancy.

A value of less than 1.0 ev for the diffusion of radiation induced vacancies is not surprising when the value is compared to the values for vacancy diffusion found by Watkins and Corbett in electron irradiated silicon.[15,16] They found an activation energy for vacancy motion of 0.33 $\pm$ 0.03 ev. They observed a divacancy which had an activation energy for motion of about 1.3 ev and a binding energy greater than 1.5 ev. The vacancy produced two energy levels, one above and one below the middle of the forbidden band. The divacancy exhibited essentially the same energy levels as the vacancy with the addition of another level deep in the forbidden band. They were unable to observe

---

[12] S. Mayburg and L. Rotondi, Phys. Rev. 91, 1015 (1953).

[13] R. A. Logan, Phys. Rev. 101, 1455 (1956).

[14] P. Baruch, J. Appl. Phys. 32, 653 (1961).

[15] G. D. Watkins and J. W. Corbett, Discussions of the Faraday Society 31, 86 (1961).

[16] G. D. Watkins, International Conference on Crystal Lattice Defects, September 1962. Kyoto, Japan.

the presence of an interstitial.

The level at 0.2 ev below the conduction band has generally been attributed to the interstitial. The work of Baruch shows the defect to have a negative charge.[17] Additional evidence suggesting that the 0.2 ev level is due to a vacancy has been reported by Logan.[18] He found one electron acceptor level at about 0.2 ev below the conduction band in quenched n-type germanium. Quenching is generally thought to produce vacancies.

These data indicate that the electrically active defect is the vacancy and that the annealing mechanism involves the impurity atom. It therefore seems reasonable to consider a mechanism involving an antimony-vacancy complex. The most stable complex might then be the antimony-divacancy.

D. Antimony-Vacancy and Antimony-Divacancy Model

A possible model involving an antimony-vacancy complex and an antimony-divacancy complex would consist of three parallel processes.

1. A vacancy may diffuse to a lattice site adjacent to an antimony atom forming an antimony-vacancy complex. The rate constant for the reaction k_1 would be a function of the activation energy for motion of the vacancy (E_m). There is a finite probability of dis-association of the antimony-vacancy complex. The rate constant k_2 for the break up of the complex would be proportional to the sum of the bind-

---

[17] P. Baruch, op. cit.

[18] R. A. Logan, Phys. Rev. 101, 1455 (1956).

ing energy E_1 and the energy of motion. The reaction may be written

$$V + Sb \underset{k_2}{\overset{k_1}{\rightleftharpoons}} SbV$$

where V denotes a vacancy, Sb an antimony atom and SbV an antimony-vacancy complex.

2. Since there is a binding energy for a divacancy, the antimony-vacancy complex may capture a second vacancy to form an antimony-divacancy complex. Although the capture cross section is different from that of antimony-vacancy formation, the rate constant k_3 will still be a function of the energy of motion, E_m. The probability for breakup of the antimony-divacancy (SbV_2) is a function of the sum of the energy for motion and the binding energy of the divacancy. One can infer from the data on silicon that the divacancy binding energy is quite high. Hence the SbV_2 complex can be stable and the rate constant for breakup assumed to be zero. The reaction for this process becomes

$$V + SbV \xrightarrow{k_3} SbV_2$$

3. A vacancy may diffuse to an annihilation site such as a surface or a jog in a dislocation line and be removed from the lattice. A typical dislocation line density for low dislocation line density germanium is of the order of 10^4 cm^{-3}. If one assumes a jog in the line at every tenth lattice site, the concentration of annihilation sites due to such dislocation lines is given by

$$\frac{10^4}{5.62 \times 10^{-7}} \sim 2 \times 10^{10} .$$

This is about four orders of magnitude lower than the concentration of introduced vacancies, however, these sites are not saturable. The capture of a vacancy results in a displacement of a section of the line but does not remove the line or change the number of jogs. The capture cross section will be different from those of processes 1 and 2, but again the rate constant k_4 will be a function of the energy for motion of a vacancy. The reaction for this process becomes

$$V \xrightarrow{k_4} 0,$$

where 0 denotes annihilation.

Denoting the concentration of each species by N with a subscript, the following differential equations may be written

$$\text{(a)} \quad \frac{dN_V}{dt} = - k_1 N_V N_{Sb} + k_2 N_{SbV} - k_3 N_V N_{SbV} - k_4 N_V$$

$$\text{(b)} \quad \frac{dN_{Sb}}{dt} = - k_1 N_V N_{Sb} + k_2 N_{SbV}$$

$$\text{(c)} \quad \frac{dN_{SbV}}{dt} = k_1 N_V N_{Sb} - k_2 N_{SbV} - k_3 N_V N_{SbV}$$

$$\text{(d)} \quad \frac{dN_{SbV_2}}{dt} = k_3 N_V N_{SbV}$$

The equation of conservation for the impurity atoms is given by

$$\text{(e)} \quad N_{Sb} + N_{SbV} + N_{SbV_2} = N_{Sb}^{o}$$

Equations a, b, c, d, have not been solved in this form. One can, however, make some simplifying assumptions based on the system under study.

The rate of interaction between the vacancies and the ith type center is given by the product $\varphi_V \sigma_i N_i$ where

φ_V is the flux of vacancies,

σ_i is the cross section for the interaction, and

N_i is the concentration of the i th type center.

The flux φ_V is the number of vacancies crossing a unit area per unit time.

If P is the probability per second that a vacancy will make a jump to an adjacent site, then the probability for a jump in any direction is $\frac{1}{3}$ P. The number of lattice sites immediately adjacent to a given area is $\frac{1}{d^2}$ where d is the distance between atoms. The fraction of these sites which will be occupied by vacancies is given by $\frac{N_V}{N}$ where N is the concentration of lattice sites. The number crossing an arbitrary area per second in a positive direction N_V^+ is then given by

$$N_V^+ = \frac{1}{2}\frac{P}{3}\frac{1}{d^2}\frac{N_V}{N} .$$

The total vacancy flux φ_V is then given by

$$\varphi_V = N_V^+ + N_V^- = \frac{1}{3}\frac{P}{d^2}\frac{N_V}{N} .$$

The concentration of lattice sites N is determined by the lattice distance d. $N = \frac{\beta}{d^3}$, where β is a constant of the order of unity.

$$\varphi_V = \frac{1}{3} d\, N_V\, P.$$

The value of P is given by

$$P = \nu\, e^{-E_m/kT}$$

where ν is the lattice vibration frequency,

E_m is the activation energy for motion, and

k is the Boltzman constant.

The vacancy flux then becomes

$$\varphi_V = \frac{1}{3} \; d \; N_V \; \nu \; e^{-E_m/kT} \; .$$

The rate of capture of vacancies at antimony sites is the product of the cross section for capture of a vacancy by an antimony atom, σ_{Sb}, the concentration of antimony atoms, and the flux. Hence, the reaction for vacancy capture by antimony atoms can be written

$$k_1 \; N_V \; N_{Sb} = \sigma_{Sb} \; N_V \; N_{Sb} \; \frac{1}{3} \; d \; \nu \; e^{-E_m/kT} \; .$$

The rate at which the antimony vacancy complex supplies free vacancies back to the lattice is given by

$$k_2 \; N_{SbV} \; .$$

From the principle of detailed balancing, the following equation can be written:

$$k_2 \; N_{SbV} = k_1 \; N_V \; N_{Sb} \; .$$

Hence, k_2 is given by

$$k_2 = k_1 \frac{N_V \; N_{Sb}}{N_{SbV}} = \frac{1}{3} \; d \; \nu \; \sigma_{Sb} \; \frac{N_V \; N_{Sb}}{N_{SbV}} \; e^{-E_m/kT} \; .$$

At equilibrium the concentration ratio is given by

$$\frac{N_V \; N_{Sb}}{N_{SbV}} = \text{constant} = \frac{N}{\omega} \; e^{-E_1/kT} \; .$$

The parameter ω is the number of ways the vacancy can escape the complex. Since there are four adjacent lattice sites, the value of ω is 4. The expression for k_2 then becomes

$$k_2 = \frac{1}{12} d \nu \sigma_{Sb} N e^{-(E_m + E_1)/kT} .$$

The rate of capture of vacancies at antimony-vacancy sites is given by

$$k_3 N_V N_{SbV} = \frac{1}{3} d N_V N_{SbV} \sigma_{SbV} \nu e^{-E_m/kT}$$

The rate of vacancy capture at dislocation lines is

$$k_4 N_V = N_V N_o \sigma_o \frac{d}{3} \nu e^{-E_m/kT} .$$

The rate constants can be written in terms of vacancy motion and the respective interaction

$$k_1 = \sigma_{Sb} \frac{d}{3} \nu e^{-E_m/kT} ,$$

$$k_2 = \frac{d}{12} \nu \sigma_{Sb} N e^{-(E_m + E_1)/kT} ,$$

$$k_3 = \sigma_{SbV} \frac{d}{3} \nu e^{-E_m/kT} , \text{ and}$$

$$k_4 = N_o \sigma_o \frac{d}{3} \nu e^{-E_m/kT} .$$

One may consider the magnitude of the reactions involved in the model using the expressions for the rate constants. In the vacancy-antimony reaction these expressions are given by

$$k_1 N_V N_{Sb} = N_V N_{Sb} \sigma_{Sb} \frac{d}{3} \nu e^{-E_m/kT} , \text{ and}$$

$$k_2 N_{SbV} = \frac{d}{12} \nu \sigma_{Sb} N_{SbV} N e^{-(E_m + E_1)/kT} .$$

In the vacancy-antimony-divacancy reaction it is given by

$$k_3 N_V N_{SbV} = N_V N_{SbV} \sigma_{SbV} \frac{d}{3} \nu e^{-E_m/kT} .$$

The cross sections are functions of the ranges of the interaction forces. These forces are the coulomb forces and the forces resulting from lattice strain.

The coulomb force is attractive in the case of σ_{Sb}, but it would be negative or zero in the case of σ_{SbV} and σ_o. The value of N_{Sb} is of the order of 10^{14}. The value of N_o is of the order of 10^{10}. Consequently, one can write the inequality:

$$k_1 N_V N_{Sb} >> k_4 N_V .$$

The vacancy concentration is less than half the antimony concentration. Consequently N_{SbV} can never under any condition be as great as N_{Sb}. If the charge of the antimony-vacancy were zero, the cross section for the capture of a second vacancy would be determined by the range of the lattice strain. This range should be of the order of 5 Å. The range of the electric field of a charge is of the order of 20 Å. If the SbV is negatively charged, a repulsion would result.

The ratio of the rate of formation of antimony-vacancy complexes to the rate of formation of antimony-divacancy complexes is given by

$$\frac{k_1 N_V N_{Sb}}{k_3 N_V N_{SbV}} = \frac{\sigma_{Sb} N_{Sb}}{\sigma_{SbV} N_{SbV}} .$$

The ratio of the cross sections is given by

$$\frac{\sigma_{Sb}}{\sigma_{SbV}} \sim \left(\frac{20 \times 10^8}{5 \times 10^8}\right)^2 = 16 .$$

The principle of detailed balancing gives

$$\frac{N_V N_{Sb}}{N_{SbV}} = \text{const} = \frac{N}{\omega} e^{-E_1/kT} .$$

Hence

$$\frac{N_{Sb}}{N_{SbV}} = \frac{N}{\omega\ N_V}\ e^{-E_1/kT}$$

N is 4.45×10^{22} cm^{-3}. N_V is approximately 5×10^{13} cm^{-3}. For E_1 = 0.5 ev, the ratio of concentrations becomes

$$\frac{N_{Sb}}{N_{SbV}} = \frac{4.45 \times 10^{22} \times 10^{-6}}{4 \times 0.5 \times 10^{14}} \approx 2 \times 10^2$$

Hence

$$\frac{k_1\ N_V\ N_{Sb}}{k_3\ N_V\ N_{SbV}} = 16 \times 2 \times 10^2 \approx 3 \times 10^3 .$$

The ratio of the rate of breakup of antimony-vacancy complexes to the rate of formation of antimony-divacancies is given by

$$\frac{k_2\ N_{SbV}}{k_3\ N_V\ N_{SbV}} = \frac{\sigma_{Sb}}{\sigma_{SbV}}\ \frac{N}{N_V}\ \frac{1}{4}\ e^{-E_1/kT} .$$

If one assumes E_1 to have a value of 0.5 ev or less, the ratio becomes

$$\frac{k_2\ N_{SbV}}{k_3\ N_V\ N_{SbV}} = 16 \times \frac{4.45 \times 10^{22}}{5 \times 10^{13}} \times \frac{1}{4} \times 10^{-6} \approx 3.2 \times 10^3 .$$

Thus the process of formation and breakup of antimony-vacancy complexes is much more rapid than the other two processes if the assumption that E_1 is not greater than 0.5 ev is valid.

It was pointed out by Robinson that the differential equations might be solvable if the first process was dominant such that one could assume a quasi equilibrium.[19] The considerations of the individual reactions indicate that this is a reasonable assumption. The validity

---

[19] M. T. Robinson, private communication.

of the assumption is also supported by the annealing data.

The isochronal anneal, Figure 7, showed a complex anneal in the temperature range below 395°K. There was an early anneal in the total state concentration followed by a plateau up to 395°K. The deep state concentration had a pronounced minimum at about 360°K. This indicates that some new process becomes dominant at about 360°K.

If the assumption is made that the first process comes to a rapid quasi equilibrium in an isothermal anneal, then one may write

$$\text{(f)} \quad k_1 N_V N_{Sb} \simeq k_2 N_{SbV} \ .$$

This implies that $\frac{d N_{Sb}}{dt}$ is approximately zero and that the free antimony concentration N_{Sb} remains constant once the quasi equilibrium expressed by (f) is established.

As a consequence of (f) substituted into (b), one can write

$$N_{Sb} = N_{Sb}^{*} \ .$$

The asterisk is used to designate the concentration at the time the equilibrium is established.

The remainder of the anneal will now be considered with the establishment of N_{Sb}^{*} as the beginning of the anneal.

The initial vacancy concentration becomes

$$N_V^{*} = N_V^{o} - N_{SbV}^{*}$$

where N_V^{o} is the vacancy concentration introduced by the irradiation.

Equation (f) may be written as

$$\text{(f')} \quad k_1 N_V N_{Sb}^{*} = k_2 N_{SbV} \ .$$

The principal annealing process will be considered to begin at the establishment of the equilibrium. At the beginning of the principal anneal, ($t = t_o$), the expression becomes:

$$(f'') \quad k_1 N_V^* N_{Sb}^* = k_2 N_{SbV}^*$$

Equation (f'') is an equilibrium equation in which N_V^* and N_{SbV}^* are the initial values. The concentration of vacancies and the antimony-vacancy concentration will change as the anneal proceeds.

Substituting (f') into (c) one obtains:

$$\frac{d\, N_{SbV}}{dt} = - \frac{k_2\, k_3}{k_1\, N_{Sb}^*} N_{SbV}{}^2 \quad .$$

Thus N_{SbV} behaves according to a second order law. Solving subject to the condition that $N_{SbV} = N_{SbV}^*$ at $t = t_o$, one obtains for the time dependence of the antimony vacancy complex:

$$(g) \quad N_{SbV} = \frac{k_1\, N_{Sb}^*\, N_{SbV}^*}{N_{SbV}^*\, k_2 k_3\, t + k_1\, N_{Sb}^*} \quad .$$

Comparing equations (c) and (d) subject to the assumption of equation (f') one can see at once that:

$$\frac{d}{dt} N_{SbV_2} = - \frac{d}{dt} N_{SbV} \quad .$$

Assuming that the rate of annihilation is slow, the antimony divacancy concentration is given by

$$N_{SbV_2} = - N_{SbV} + K \ .$$

Since at $t = t_o$,

$$N_{SbV_2} = N_{SbV_2}^* \quad ,$$

then,

$$K = N^*_{SbV_2} + N^*_{SbV} \quad .$$

The expression for N_{SbV_2} then becomes

$$\text{(h)} \quad N_{SbV_2} = \frac{(N^*_{SbV})^2 \quad k_2 \quad k_3 \quad t}{N^*_{SbV} \quad k_2 k_3 t + k_1 \; N^*_{Sb}} + N^*_{SbV_2} \quad .$$

As t approaches infinity, equation (h) has a limiting value of $N^*_{SbV} + N^*_{SbV_2}$. Under these conditions eq. (a) has the limiting form:

$$\frac{d \; N_V}{dt} = - \; (k_3 \; N_{SbV} + k_4) \; N_V \quad .$$

Hence:

$$\frac{d \; N_V}{V} = - \; (k_3 \; N_{SbV} + k_4) \; dt \quad .$$

Integrating, one obtains:

$$\ln N_V = K' - k_4 t - \int k_3 \; N_{SbV} \; dt \quad .$$

Substituting for N_{SbV} from eq. (h), the integral term becomes

$$\int \frac{k_1 \; k_3 \; N^*_{Sb} \; N^*_{SbV} \; dt}{k_2 \; k_3 \; N^*_{SbV} \; t + k_1 \; N^*_{Sb}}$$

which becomes on integration:

$$\frac{k_1}{k_2} \; N^*_{Sb} \quad \ln \; (k_2 \; k_3 \; N^*_{SbV} \; t + k_1 \; N^*_{Sb}) + K'' \quad .$$

K'' and K' can be combined into a constant $\ln K_o$.

Taking the antilog and solving K_o subject to the condition that

$$N_V = N^*_V$$

at $t = t_o$,

one obtains for $\ln K_o$,

$$\ln K_o = \ln N_V^* + \frac{k_1}{k_2} N_{Sb}^* \ln k_1 N_{Sb}^* .$$

Using this value for $\ln K_o$, the value of N_V becomes:

$$N_V = N_V^* \; e^{-k_4 t} \left[1 + \frac{k_2 \; k_3 \; N_{SbV}^*}{k_1 \; N_{Sb}^*} t \right]^{-\frac{k_1}{k_2} N_{Sb}^*} .$$

From the equilibrium condition

$$k_1 \; N_V^* \; N_{Sb}^* = k_2 \; N_{SbV}^* ,$$

the second term in the brackets reduces to $k_3 \; N_V^*$. The value of N_V^* is less than 10^{14}. The value of k_3 is given by

$$k_3 = \sigma_{SbV} \frac{d}{3} \; \nu \; e^{-E_m/kT} .$$

Using E_m = 1 ev and a temperature of 350°K, the exponential becomes 10^{14}. Hence the order of magnitude of $k_3 \; N_V^*$ becomes:

$$k_3 \; N_V^* \simeq 2.5 \times 10^{-15} \times 10^{-8} \times 10^{14} \times 10^{-14} \times 10^{14} \simeq 10^{-9} .$$

Consequently for times short compared to 10^9 sec, the bracketed factor may be expressed as an exponential. It reduces to $e^{-k_3 \; N_{SbV}^* t}$. Hence N_V becomes:

$$\text{(i)} \quad N_V = N_V^* \; e^{-(k_3 \; N_{SbV}^* + k_4) \; t} .$$

The measured quantity in the experiment is the carrier concentration. The carrier concentration is related to the charge centers according to

$$n = \sum_i I_i \; N_i .$$

where n is the carrier concentration,

N_i is the concentration of the i th type charge center, and

I_i is the ionization state of the i th type charge center.

Prior to irradiation to the carrier concentration was due to the antimony concentration. Since $I = 1$ in this case,

$$n_o = N_{Sb}^o \quad .$$

As a consequence of irradiation, centers which are assumed to be vacancies are introduced. It can be seen in Figure 26 that at least two ionization states are present, one ionization level occurring at about 0.2 ev below the lower edge of the conduction band. The dependence of carrier removal on irradation is shown in Figure 25. The carrier concentration change is shown for measurements at 77^oK and 273^oK. Hence, the measurements of carrier concentration are taken with the Fermi level in the sample above the 0.2 ev level for the 77^oK reading and below the 0.2 ev level for the 273^oK reading. The ratio of the introduction rate as measured at these two temperatures is 2:1. Thus one can assume that the defect is singly charged at 273^oK and doubly charged at 77^oK. In this model, the ionization state of the interstitial, I_I, is taken as zero.

The function plotted is $f(n)$ which is given by:

$$f(n) = \frac{n_o - n_t}{n_o - n_r} \quad ,$$

where $n_o = N_{Sb}^o$,

$n_r = N_{Sb}^o - I_V N_V^o$, and

$n_t = N_{Sb}^o - I_V N_V - I_c N_{SbV} - I_d N_{SbV_2}$.

Hence:

$$n_o - n_t = I_V N_V + I_c N_{SbV} + I_d N_{SbV_2} \text{ , and}$$

$$n_o - n_r = I_V N_V^o \text{ .}$$

The value for f(n) becomes:

$$f(n) = \frac{1}{I_V N_V^o} \left\{ I_V N_V + I_c N_{SbV} + I_d N_{SbV_2} \right\} .$$

Substituting the derived expressions for the concentration, f(n) becomes:

$$\text{(j)} \quad f(n) = \frac{1}{I_V N_V^o} \left\{ I_V N_V^* e^{-(k_3 N_{SbV}^* + k_4) t} + \frac{I_c k_1 N_{Sb}^* N_{SbV}^*}{N_{SbV}^* k_2 k_3 t + k_1 N_{Sb}^*} + \frac{I_d (N_{SbV}^*)^2 k_2 k_3 t}{N_{SbV}^* k_2 k_3 t + k_1 N_{Sb}^*} + I_d N_{SbV_2}^* \right\} .$$

The value for the plateau is obtained by letting t become large. It is given by:

$$\text{(k)} \quad f(n)_\infty = \frac{I_d (N_{SbV}^* + N_{SbV_2}^*)}{I_V N_V^o} .$$

The saturation plateau is obtained from the antimony divacancy terms. The bracketed factor is precisely the value of N_{SbV_2} as t becomes large.

One can infer from the irradiation carrier removal as a function of temperature, Figure 25, and the change in Hall constant with temperature, Figure 26, that the value of I_V changes from one to two as the

Fermi level moves from below the 0.2 ev level to a position above the 0.2 ev level. Hence:

$I_V = 1$ for $T = 273^oK$, and

$I_V = 2$ for $T = 77^oK$.

The plateau values are then given by:

$$f(n)_{273} = \frac{I_d\ (273)\ (N^*_{SbV} + N^*_{SbV_2})}{N^o_V}\ , \text{ and}$$

$$f(n)_{77} = \frac{I_d\ (77)\ (N^*_{SbV} + N^*_{SbV_2})}{2\ N^o_V}\ .$$

Taking the ratio one obtains:

$$\frac{f(n)_{273}}{f(n)_{77}} = 2\ \frac{I_d\ (273)}{I_d\ (77)}\ .$$

Analysis of the plateaux for the isothermal anneals indicates that the ratio of $I_d(273)$ to $I_d(77)$ is 2/3. This ratio of values for I_d implies that the antimony divacancy has three levels in the forbidden band. One level is at about 0.2 ev the other two are near or below the middle of the band. This observation is similar to the results of Watkins and Corbett in the case of silicon.[20] They found the vacancy to have two levels one above and one below the middle of the forbidden band. They found the divacancy to have three levels. Two of the levels were the same as the vacancy, the third was lower in the forbidden band.

---

[20] Watkins and Corbett, loc. cit.

Using the relation $k_1 N_V^* N_{Sb}^* = k_2 N_{SbV}^*$, eq. (j) can be expressed as:

$$(j') \quad f(n) = \frac{1}{I_V N_V^o}\left\{ I_V N_V^* e^{-(k_3 N_{SbV}^* + k_4)t} + N_{SbV}^* \left[\frac{I_c + I_d N_V^* k_3 t}{1 + N_V^* k_3 t} \right] + I_d N_{SbV_2}^* \right\} .$$

A parameter τ may be defined by:

$$\frac{1}{\tau} \equiv k_3 N_{SbV}^* + k_4 .$$

The I_i are constants at a fixed temperature hence the term $I_d N_{SbV_2}^*$ is a constant.

The value of I_c is some number such as one or two and it can be seen that $k_3 N_V^*$ has a value of about 10^{-9}. The value of 10^{-9} was obtained using a value of 1 ev for the activation energy for vacancy motion. Consequently the central term is essentially constant.

For times short compared to 10^9 seconds, the equation can be approximated by:

$$f(n) = \frac{1}{I_V N_V^o} \left\{ I_V N_V^* e^{-t/\tau} + I_c N_{SbV}^* + I_d N_{SbV_2} \right\} .$$

But,

$$N_V^* \equiv N_V^o - N_{SbV}^* .$$

Hence:

$$f(n) = \left(1 - \frac{N_{SbV}^*}{N_V^o}\right) e^{-t/\tau} + \frac{I_c}{I_v} \frac{N_{SbV}^*}{N_V^o} + \frac{I_d}{I_v} \frac{N_{SbV_2}}{N_V^o} .$$

Denoting $\frac{N_{SbV}^*}{N_V^o}$ by λ, one can write:

$$f(n) = (1 - \lambda)\, e^{-t/\tau} + \lambda + f_1 \quad ,$$

where f_1 includes the change in f(n) due to the Reiss type anneal as well as the small term $\frac{I_d}{I_V} \frac{N^*_{SbV_2}}{N^o_V}$, and the error due to assuming $I_c = I_d$.

The value of τ is determined from the half point of the annealing curve.

The saturation plateau is $\lambda + f_1$. The value of λ chosen for curve fitting will change with the choice of f_1.

A set of curves calculated from this approximate expression for 77^oK and two choices of f_1 is shown in Figure 27. The corresponding experimental points are also plotted. Since no attempt was made to include the details of the early anneal, the discrepancy for times before equilibrium in f_1 is established is to be expected.

The derived expression fits the experimental data satisfactorily. The equation is approximately first order in form. This equation can be extended to the 273^oK measurement as well as the difference measurements. The value of $\tau_{\frac{1}{2}}$ for all three conditions of measurement is plotted as a function of reciprocal temperature in Figure 21. The activation energies that one could measure from Figure 21 would be essentially the same for all three conditions of measurement.

The saturation plateau is $f(n)_\infty + f_1$. This is given by:

$$\frac{I_d}{I_V\ N^o_V} (N^*_{SbV} + N^*_{SbV_2}) + R \quad ,$$

where R is the fraction of the anneal produced by the Reiss process. R is a function of the impurity density and the defect densities.

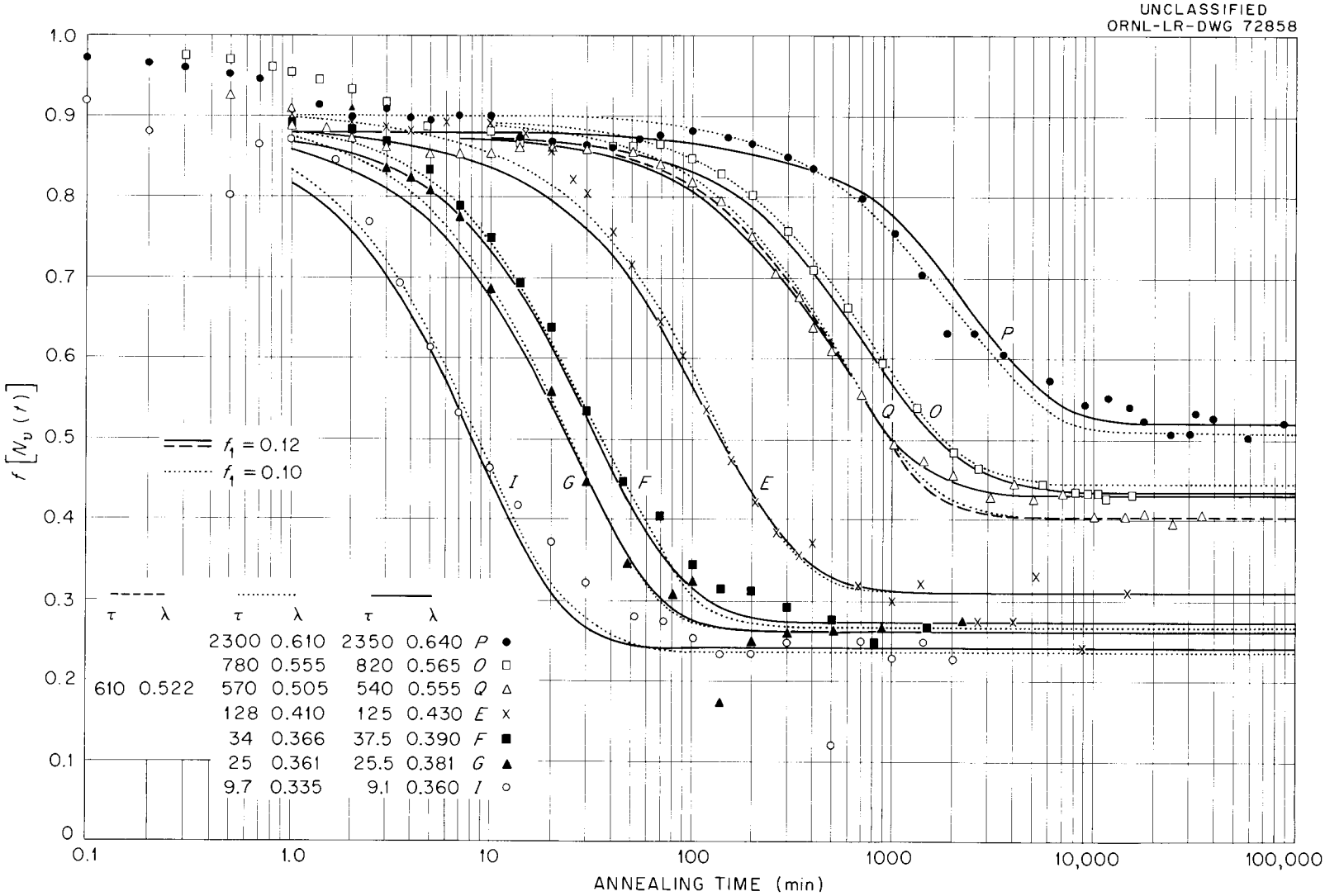

Figure 27. Fit of data by an approximated equation.

These are similar from sample to sample since all samples were cut from the same ingot and irradiated to about the same change in carrier concentration. The complex $N^*_{SbV_2}$ is produced by a reaction much slower than that producing N^*_{SbV}. In addition the N_{SbV_2} reaction is second order and involves N^*_{SbV}. The variation in the saturation plateau is then a function of the variation in N^*_{SbV}.

From the equilibrium expression, one can write:

$$N^*_{SbV} = \frac{k_1}{k_2} N^*_{Sb} N^*_V \quad .$$

Substituting the values of k_1 and k_2 the expression becomes:

$$N^*_{SbV} = \frac{4}{N} e^{E_1/kT} N^*_{Sb} N^*_V \quad .$$

Hence λ is given by

$$\lambda = 4 \frac{N^*_{Sb} N^*_V}{N N^o_V} e^{\frac{E_1}{kT}} \quad .$$

The logarithm is given by

$$\ln \lambda = \frac{E_1}{kT} + \ln \frac{4 N^*_{Sb} N^*_V}{N N^o_V} \quad .$$

The value of λ depends upon the assumption of f_1. However at low temperatures, the temperature dependence of the saturation plateau will be dominated by the E_1/kT contribution. A plot of the log of the plateaux vs $10^3/T$ is shown in Figure 10. Analyzing the low temperature section by the techniques such as are used to separate radioactive decay times, one finds a value for E_1 of 0.385 ev.

The parameter τ is given by the expression:

$$\frac{1}{\tau} = k_3 N^*_{SbV} + k_4 \quad .$$

Substituting for N^*_{SbV} one obtains:

$$\frac{1}{\tau} = k_3 \frac{k_1}{k_2} N^*_{Sb} N^*_V + k_4 .$$

Substituting for the k_s one obtains:

$$\frac{1}{\tau} = N^*_{Sb} N^*_V \sigma_{SbV} \frac{4}{3} \frac{d \nu}{N} e^{-(E_m - E_1)/kT}$$

$$+ N_o \sigma_o \frac{d}{3} \nu e^{-E_m/kT} .$$

The first term will dominate in the high temperature range, the second term will dominate in the low temperature range. Although Figure 9 is not as amenable to separation for activation energy analysis as is Figure 10, the difference in slopes in Figure 9 indicates a value of E_1 of 0.334 ev which compares to 0.385 ev from Figure 10.

The approximations used in the model involved a choice of an upper limit of 0.5 ev for E_1. A value of 0.4 ev is below the limit imposed.

The formation of the antimony vacancy complex converts isolated charge centers to dipoles. This can account for the observed change in mobility without a change in the total state concentration.

The increase in deep state concentration after the minimum in the isochronal anneal can be attributed to two factors. One is the break up of antimony vacancy complexes as the temperature is increased. The second is the formation of divacancies which introduces an additional deep level.

E. Other Possible Models

The observed activation energy for defect motion seems to rule out any model which depends upon interstitials alone. The available information requires a dependence upon impurity concentrations and hence rules out models which depend upon vacancies, or vacancy-interstitial interactions which do not involve the impurity atom. The formation of the plateau requires one complex which is stable to annealing at the temperatures used here. This rules out all models which do not have some mechanism to produce a stable complex.

One possible model would be one in which the vacancy and antimony interact to form an antimony-vacancy complex. The antimony vacancy complex would reduce the coulomb-barrier such that an interstitial could diffuse to the SbV complex. The complex could then be removed in three ways,

1. The complex could decompose to a free antimony and a free vacancy.
2. The complex could capture a second vacancy to produce an antimony divacancy.
3. The complex could capture an interstitial resulting in a vacancy interstitial annihilation.

The impurity-vacancy-interstitial model is attractive. However, until some method of detecting interstitials is available there is no way of checking on the model.

F. The 0.09 ev Level

The model does not explain the presence of the 0.09 ev level.

Since this level does not anneal, it is possible that it is the result of some Reiss type capture of defects on some impurity such as oxygen or copper which may be present in the sample. The level may also be due to interstitial clusters which could be formed at low temperature due to the high suspected mobility of the interstitial. There is no information available to identify this level. It is produced by the early anneal but does not change on further anneal. Thus it is assumed that the defect producing the 0.09 ev level is not involved in the major annealing process.

The 0.09 ev level in germanium is similar to the 0.17 ev level in silicon which has been identified by Watkins and Corbett as a vacancy trapped by an interstitial oxygen.[21]

---

[21] G. D. Watkins and J. W. Corbett, Phys. Rev. 121, 1001 (1961).

CHAPTER V

SUMMARY

The principal result of this study is to point up the details in the kinetic processes involved in the annealing of radiation induced defects. The observations are consistent with the assumption that the defect introduced which dominates the change in the electron concentration in n-type germanium behaves like a vacancy.

The annealing kinetics are controlled by the vacancy impurity interaction and thus the type of impurity as well as its concentration.

Although the values of the rate constants are not completely determined, some information as to their relative size and respective temperature dependence can be deduced.

The model proposed produces an expression which accounts for the observed behavior. Some simplifying assumptions applied to the derived expression result in an equation which is amenable to data fitting.

The model proposed for antimony as the impurity is as follows:

1. $V + Sb \underset{k_2}{\overset{k_1}{\rightleftharpoons}} SbV$

2. $V + SbV \xrightarrow{k_3} SbV_2$

3. $V \xrightarrow{k_4} 0$

The experimental data indicates that the antimony-vacancy interaction and antimony vacancy decomposition are the dominating processes

and that these reactions are orders of magnitude faster than the antimony-divacancy formation or the vacancy annihilation process. Hence process (1) comes to rapid equilibrium. This model leads to the following expression for the fraction of induced defect concentration remaining after anneal

$$f(n) = \frac{1}{I_V \; N_V^o} \left\{ I_V \; N_V^* \; e^{-(k_3 \; N_{SbV}^* + k_4)\, t} + N_{SbV}^* \left[\frac{I_c + I_d \; N_V^* \; k_3 t}{1 + N_V^* \; k_3 t} \right] + I_d \; N_{SbV_2}^* \right\} + f_1$$

where f_1 is the fraction removed by means of the process proposed by Reiss.

The resultant expression can be simplified by approximation to a form that is readily compared with the experimental data. The comparison shows good agreement within the limits of the approximations imposed.

Although the activation energy indicated by the annealing may be correlated with the activation energy for vacancy motion, the annealing is not a simple process and hence the usual graphical techniques for activation energy analysis do not give a unique value. The values of the activation energy may be determined by such techniques, to a good approximation, if one makes the proper choice for the impurity concentration and the temperature of anneal. The activation energy for motion of the vacancy is found to be 0.8 ev. The binding energy of the

antimony complex is 0.4 ev.

The data reported here has led to an analysis which has uncovered a few facts that explain the observations of the general behavior of annealing in germanium. New questions, however, have been raised. The dependence of the nature of the induced defect on the temperature of the sample during irradiation, is perhaps the next area to be studied. A series of annealing experiments should be conducted using a wide range of impurity concentrations as well as concentration of radiation induced defects.

Another experiment which is suggested by these results is the study of the annealing of the saturation plateau. This would involve irradiating a series of samples under the same conditions used in this study. A postirradiation Hall-effect curve would then be measured as a function of temperature. The samples would then be annealed at 380°K to produce the saturation plateau condition. The plateau would then be annealed using the techniques of isochronal and isothermal annealing. This experiment would yield the binding energy of the antimony divacancy complex.

The true nature of the apparent annealing between liquid nitrogen temperature and 273°K needs further study. The large change exhibited by the reciprocal mobility upon warming the sample to ice temperature suggests that the mechanism may involve more than simply the emptying of traps. Isochronal and isothermal anneals in this temperature range could be conducted in the dark. The sample could then be illuminated and then re-measured. The illumination would fill the traps and the heating would

produce no change if true annealing had not occurred.

The question of the presence of interstitial might be resolved from a study of the dependence of the dielectric constant on crystal orientation. The antimony-vacancy complex dipole as well as a di-vacancy must be orientated along the direction of the crystal bond. An interstitial pair will be orientated in the direction of the lattice voids. The change in the dielectric constant as a function of irradiation and anneal of samples cut along different crystallographic planes might indicate the presence of interstitial pairs.

BIBLIOGRAPHY

A. BOOKS

Billington, D. S. and J. H. Crawford, Jr., Radiation Damage in Solids (Princeton University Press, Princeton, 1961).

Dunlap, W. Crawford, Jr., An Introduction to Semiconductors (John Wiley and Sons, Inc., New York, 1957).

Frost, Arthur A. and Ralph G. Pearson, Kinetics and Mechanisms (John Wiley and Sons, Inc., New York, 1958).

Shockley, W., Electrons and Holes in Semiconductors (D. Van Nostrand Company, New York, 1958).

B. PERIODICALS

Baruch, P., J. Appl. Phys. 32, 653 (1961).

Bate, R. T. and A. E. Beer, J. Appl. Phys. 32, 806 (1961).

Blount, E. I., J. Appl. Phys. 30, 1218 (1959).

_____, Phys. Rev. 113, 995 (1959).

Brown, W. L. and W. M. Augustyniak, J. Appl. Phys. 30, 1300 (1959).

_____, W. M. Augustyniak, and J. R. Waite, J. Appl. Phys. 30, 1258 (1959).

_____, R. C. Fletcher, and K. A. Wright, Phys. Rev. 92, 591 (1953).

Cleland, J. W., J. H. Crawford, Jr., and D. K. Holmes, Phys. Rev. 102, 722 (1956).

Conwell, E. M., Proc. IRE 40, 1327 (1952).

Crawford, J. H. Jr. and J. W. Cleland, J. Appl. Phys. 30, 1204 (1959).

Curtis, O. L. Jr. and J. H. Crawford, Jr., Phys. Rev. 126, 1342 (1962).

Debye, P. P. and E. M. Conwell, Phys. Rev. 93, 693 (1954).

Gossick, B. R., J. Appl. Phys. 30, 1214 (1959).

Haiman, G. C. and T. Higier, J. Appl Phys. 33, 2198 (1962).

Haynes, J. R. and J. A. Hornbeck, Phys. Rev. 90, 152 (1953).

Hobstetter, J. N. and C. A. Renton, J. Appl Phys. 33, 600 (1962).

James, H. and K. Lark-Horovitz, Z. Physik. Chem. 198, 107 (1951).

Klontz, E. E. and J. W. MacKay, Bull. Amer. Phys. Soc. Series II, 6, 303 (1961).

Loferski, J. J. and P. Pappaport, J. Appl. Phys. 30, 1296 (1959).

Logan, R. A., Phys. Rev. 101, 1455 (1956).

Letaw, H. Jr., W. M. Portnoy, and L. Slifkin, Phys. Rev. 102, 892 (1956).

_____, L. M. Slifkin, and W. M. Portnoy, Phys. Rev. 93, 892 (1954).

MacKay, J. W. and E. E. Klontz, J. Appl. Phys. 30, 1269 (1959).

Mayburg, S. and L. Rotondi, Phys. Rev. 91, 1015 (1953).

Oen, O. S. and D. K. Holmes, J. Appl. Phys. 30, 1289 (1959).

Reiss, H., J. Appl. Phys. 30, 1141 (1959).

Shulman, R. G., Phys. Rev. 102, 1451 (1956).

Watkins, G. D. and J. W. Corbett, Discussions of the Faraday Society 31, 86 (1961).

_____ and J. W. Corbett, Phys. Rev. 121, 1001 (1961).

C. COLLECTIONS

Dunlap, W. C. Jr., "Impurities in Germanium," Progress in Semiconductors A. F. Gibson (ed.) Vol 2 (John Wiley and Sons, Inc., New York 1957).

Fan, H. Y. and K. Lark-Horovitz, "Irradiation of Semiconductors," Semiconductors and Phosphors, M. Schön and H. Welker (eds.) (International Science Publishers, Inc., New York, 1958).

Hobstetter, J. N., "Effects of Imperfections on Germanium and Silicon," Semiconductors, N. B. Hannay (ed.) (Reinhold Publishing Company, New York, 1959).

D. REFERENCES TO BE PUBLISHED

MacKay, J. W. and E. E. Klontz, Symposium on Radiation Damage in Solids and Reactor Materials, Venice, Italy, May 1962.

Ishino, S., F. Nakazawa, and R. R. Hasiguti, "Annealing of Gamma Ray Irradiated n-type Germanium."

ORNL-3443
UC-40 — Radiation Effects on Materials
TID-4500 (19th ed., Rev.)

INTERNAL DISTRIBUTION

1. Biology Library
2-3. Central Research Library
4. Reactor Division Library
5-6. ORNL — Y-12 Technical Library
Document Reference Section
7-41. Laboratory Records Department
42. Laboratory Records, ORNL R.C.
43. J. A. Auxier
44. J. H. Barrett
45. D. S. Billington
46. R. D. Birkhoff
47. G. E. Boyd
48. J. T. Howe
49. G. S. Hurst
50. G. W. Keilholtz
51. C. E. Larson
52. W. R. Martin
53. Axel Meyer
54. W. F. Mruk
55-84. Jay Cee Pigg
85. O. E. Schow III
86. H. C. Schweinler
87. Oscar Sisman
88. M. J. Skinner
89. W. J. Stelzmann
90. J. A. Swartout
91. A. M. Weinberg
92. John Wheeler
93. H. D. Willis
94. Harvey Brooks (consultant)
95. N. Cabrera (consultant)
96. T. A. Read (consultant)
97. R. L. Sproull (consultant)
98. D. Turnbull (consultant)

EXTERNAL DISTRIBUTION

99. Research and Development Division, AEC, ORO
100-698. Given distribution as shown in TID-4500 (19th ed., Rev.) under Radiation Effects on Materials category (75 copies — OTS)